Benzoate 1,2-Dioxygenase from *Pseudomonas putida*: Single Turnover Kinetics and Regulation of a Two-Component Rieske Dioxygenase†

Matt D. Wolfe,‡,§ Daniel J. Altier,‡,|| Audria Stubna,⊥ Codrina V. Popescu,⊥,# Eckard Münck,⊥ and John D. Lipscomb*,‡

Department of Biochemistry, Molecular Biology, and Biophysics and Center for Metals in Biocatalysis, University of Minnesota, Minneapolis, Minnesota 55455, and Department of Chemistry, Carnegie Mellon University, Pittsburgh, Pennsylvania 15213

Received April 2, 2002; Revised Manuscript Received May 28, 2002

ABSTRACT: The benzoate 1,2-dioxygenase system (BZDOS) from *Pseudomonas putida* mt-2 catalyzes the NADH-dependent oxidation of benzoate to 1-carboxy-1,2-*cis*-dihydroxycyclohexa-3,5-diene. Both the oxygenase (BZDO) and reductase (BZDR) components of BZDOS have been purified and characterized kinetically and by optical, EPR, and Mössbauer spectroscopies. BZDO has an $(\alpha\beta)_3$ subunit structure in which each α subunit contains a Rieske [2Fe-2S] cluster and a mononuclear iron site. Two different purification protocols were developed for BZDO allowing the mononuclear iron to be stabilized in either the Fe(III) or the Fe(II) state for spectroscopic characterization. Using single turnover reactions, it is shown that fully reduced BZDO alone is capable of yielding the *cis*-diol product in high yield at rates that exceed the BZDOS turnover number. At the conclusion of turnover, quantification of each oxidation state of the metal sites by EPR and Mössbauer spectroscopies shows that the Rieske cluster and mononuclear iron are each oxidized in amounts equal to the product yield, suggesting that the two electrons required for catalysis derive from the two metal centers. These results are in agreement with our previous study of naphthalene 1,2-dioxygenase [Wolfe, M. D., Parales, J. V., Gibson, D. T., and Lipscomb, J. D. (2001) *J. Biol. Chem. 276*, 1945−1953], which belongs to a different Rieske dioxygenase subclass, suggesting that it is a universal characteristic of Rieske dioxygenases that oxygen activation and substrate oxidation are catalyzed by the oxygenase component alone. The EPR spectrum of the Fe(III) center after a single turnover is distinct from either of those of substrate-free or substrate-bound enzyme. The complex with this spectrum is not formed by addition of *cis*-diol product to the resting Fe(III) form of the enzyme but is observed when the Fe(II) form is oxidized in the presence of product. Together, these results suggest that product exchange occurs only when the mononuclear iron is reduced. Stopped-flow and rapid scan analyses monitoring the oxidation of the Rieske cluster during the single turnover reaction show that it occurs in three phases that are kinetically competent for catalysis. The rate of each phase was found to be dependent on the type of substrate present, suggesting that the substrate influences the rate of electron transfer between the metal clusters. The participation of substrate in the oxygen activation reaction suggests a new aspect of the mechanism of this process by the Rieske dioxygenase class.

Rieske non-heme iron dioxygenases are multicomponent systems that utilize NAD(P)H to reductively activate and cleave O_2 for incorporation into aromatic substrates to form *cis*-dihydroxylated products as illustrated for benzoate in Scheme 1. More than 50 of these enzymes have been recognized and shown to catalyze an exceptionally wide range of oxidative chemistry important for bacterial metabolism and biodegradation (*1*, *2*). They all consist of an electron transport chain utilizing flavin and [2Fe-2S] centers contained in either one or two proteins and a terminal oxygenase component. The terminal oxygenase components differ in their amino acid sequence and subunit structure, but they all contain both Rieske and mononuclear iron centers that are each essential for catalysis. Recently, a classification scheme has been introduced on the basis of the characteristics of the α subunit of the oxygenase component (*1*). Four

Scheme 1: Reaction Catalyzed by Benzoate 1,2-Dioxygenase

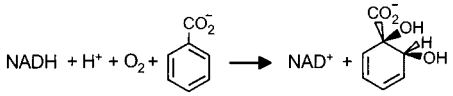

† This work was supported by National Institutes of Health (NIH) Grants GM-24689 (J.D.L.) and GM-22701 (E.M.). M.D.W. was supported in part by NIH Training Grant GM-08277.

* To whom correspondence should be addressed at the Department of Biochemistry, Molecular Biology, and Biophysics, University of Minnesota, 6-155 Jackson Hall, 321 Church St. SE, Minneapolis, MN 55455. E-mail: lipsc001@tc.umn.edu. Telephone: (612) 625-6454. Fax: (612) 624-5121.

‡ Department of Biochemistry, Molecular Biology, and Biophysics and Center for Metals in Biocatalysis, University of Minnesota.

§ Current address: Laboratory of Biochemistry, National Heart, Lung, and Blood Institute, National Institutes of Health, 2122 MSC-8012, 50 South Drive, Bethesda, MD 20892.

|| Current address: Pioneer Hi-Bred International, Inc., 7250 NW 62nd Ave., Johnston, IA 50131.

⊥ Department of Chemistry, Carnegie Mellon University.

Current address: Department of Biochemistry, Molecular Biology, and Biophysics, 6-155 Jackson Hall, University of Minnesota, Minneapolis, MN 55455.

10.1021/bi025912n CCC: $22.00
Published on Web 07/04/2002

distinct dioxygenase families emerge from this analysis and are named according to the archetypal substrate in each class: benzoate, phthalate, naphthalene, and toluene/biphenyl.

The molecular mechanism of the Rieske dioxygenase class remains unclear in terms of both the oxygen activation chemistry and regulation of the catalytic process. It is apparent from the stoichiometry of the reaction that two reducing equivalents are required. Also, spectroscopic and crystallographic studies show that the substrate binds near the mononuclear iron site on the oxygenase component, suggesting that this is the site of oxygen activation (*3*−*6*). Our recent studies of the three-component naphthalene dioxygenase system (NDOS)[1] subclass of Rieske dioxygenase show that (i) the oxygenase component (NDO) by itself is sufficient for rapid product formation in a single turnover if both the Rieske and mononuclear iron sites are reduced, (ii) the role of the ferredoxin component (NDF) in this system is to transfer electrons to the Rieske cluster and to rapidly redistribute electrons from nonfunctional to functional active sites, and (iii) the O_2 binding reaction at the mononuclear site is gated by substrate binding to the enzyme when the Rieske cluster is reduced (*7*). After one turnover, the enzyme is left with both metal sites oxidized, showing that the two electrons required for catalysis can be derived from a Rieske cluster/mononuclear iron pair. This suggests that the likely reactive oxygen species is either an Fe(III)-bound peroxo or, following O−O bond cleavage, a formal Fe(V)−oxo species. In each case, two reducing equivalents are required to form the reactive species. Somewhat different conclusions have been reached in studies of the two-component phthalate dioxygenase system (PDOS) subclass of Rieske dioxygenase. In this case, both the oxygenase (PDO) and reductase (PDR) components appear to be required for full product yield, and catalysis may require input of a reducing equivalent from the PDR in addition to the two available from the Rieske and mononuclear iron centers (*8*−*10*). Thus, the possible reactive species might include an Fe(II)−peroxo or an Fe(IV)−oxo. Following turnover in this case, the mononuclear iron site would be left in the ferrous state.

In the current study, another subclass of Rieske dioxygenase is studied, the benzoate 1,2-dioxygenase system (BZDOS) from *Pseudomonas putida* mt-2. This subclass resembles NDOS in that the oxygenase component consists of a trimer of $\alpha\beta$ protomers in contrast to the α_4 subunit structure of PDO. On the other hand, it resembles PDOS in that it has only reductase (BZDR) and oxygenase (BZDO) components and is thus missing a component comparable to the NDF component of the naphthalene dioxygenase system.

BZDOS was first purified from *P. putida* C1, and its general catalytic properties were characterized (*11*−*13*). It is shown here that the enzyme from *P. putida* mt-2 is similar in its physical and catalytic properties, but it has several advantages over this and other better studied Rieske dioxygenases that facilitate studies of the mechanism. These include the facts that (i) it can be purified in two forms with the mononuclear iron in the Fe(II) or Fe(III) state, respectively, (ii) its substrate and adventitious substrates are highly soluble, allowing the reaction to be monitored over a large range of concentration and temperature, and (iii) the electronic symmetry of the mononuclear iron site is such that EPR spectra are highly resolved and sensitive to environmental changes. Here we use this new Rieske dioxygenase system to show that the oxygenase component of a two-component Rieske dioxygenase is capable of high-yield single turnover to leave both metal centers in the oxidized state. Also, it is demonstrated that the redox state of both centers has a profound effect on the substrate binding and product release rates. Finally, it is shown that the rate of oxidation of the Rieske cluster is influenced by substrate type, which can be used to investigate the relationship between substrate binding and electron transfer.

MATERIALS AND METHODS

Chemicals. All chemicals were purchased from Sigma-Aldrich or Matheson and used without purification except for catechol, which was further purified by sublimation and stored under argon. Authentic 1-carboxy-1,2-*cis*-dihydroxycyclohexa-3,5-diene (benzoate *cis*-diol) was prepared according to a published procedure (*14*). Water was deionized and further purified using a Millipore reverse osmosis system.

Cell Growth. P. putida mt-2 (ATCC 23973), the source of BZDOS and catechol 1,2-dioxygenase (1,2-CTD) used in this study, was continually grown on modified Hutner's mineral base (MSB) (*15*) supplemented with 20 mM sodium benzoate as the sole carbon source (MSB−benzoate) to cure the strain of the TOL plasmid and specifically induce expression of 1,2-CTD and BZDOS. Removal of the TOL plasmid was required to prevent expression of toluate dioxygenase, a Rieske dioxygenase closely related to the chromosomally encoded BZDOS. MSB−benzoate was used throughout cell culture. Six 40 L carboys were inoculated with 1 L cultures, grown at room temperature, and supplemented with 3 g/L sodium benzoate after 12 and 18 h of growth. The carboys were bubbled with sterile-filtered air. After 24 h, the cells were concentrated using an Amicon DC30P ultrafiltration system and centrifuged to yield approximately 1 kg of wet cell paste, which was stored at −80 °C.

BZDOS Purification. All steps in the BZDOS purification were completed at 4 °C using standard chromatographic techniques. Two procedures were used that differed primarily in the method of stabilization of the BZDO enzyme. The steps and the yields at each step were comparable for the two procedures, so the results of only one of the procedures are summarized in Table 1.

BZDO Purification (Method I). Frozen *P. putida* cell paste (typically 500 g) was thawed and resuspended in breaking buffer (125 mM HEPES, pH 7.5, 1 mM sodium benzoate, 1 mM DTT, 5% glycerol) at a concentration of 0.5 g/mL. The cell slurry was sonicated and diluted to 500 mL with breaking buffer, and cell debris was pelleted by centrifugation for 1 h at 39000*g*. In a batch fashion, the pooled supernatant was mixed in a beaker with 200 mL of DEAE-Sepharose Fast

[1] Abbreviations: DTT, dithiothreitol; HEPES, *N*-(2-hydroxyethyl)-piperazine-*N*′-2-ethanesulfonic acid; MES, 2-(*N*-morpholino)ethanesulfonic acid; MSB, mineral salts base; BZDOS, benzoate 1,2-dioxygenase system; BZDO, oxygenase component of BZDOS; BZDR, reductase component of BZDOS; NDOS, naphthalene 1,2-dioxygenase system; NDO, oxygenase component of NDOS; NDF, ferredoxin component of NDOS; NDR, reductase component of NDOS; P450, cytochrome P450 monooxygenase; PDOS, phthalate dioxygenase system; PDO, oxygenase component of PDOS; PDR, reductase component of PDOS.

Table 1: Purification of Benzoate 1,2-Dioxygenase from *P. putida* mt-2[a]

	benzoate oxygenase				benzoate reductase			
purification step	protein (mg)	units	units/mg[b]	yield (%)	protein (mg)	units	units/mg	yield (%)
cell extract	37200	2790	0.075	100	*c*			
DEAE-Sepharose (batch)	8820	2170	0.246	78	8820	122500	13.9	100
DEAE-Sepharose	1330	1410	1.06	51	916	100800	110	82
Ultrogel AcA 34	775	1050	1.36	38				
Ultrogel AcA 44					186	94900	510	77
DEAE-Sepharose					94	74300	790	61

[a] Purification table from 500 g of wet cell paste. [b] The specific activity was determined using the standard assay without addition of Fe(II). [c] The cell extract contains NADH-dependent oxidase activity not specific for benzoate dioxygenase and was therefore not included in the purification table.

Flow resin (Pharmacia) equilibrated in buffer A (25 mM HEPES, pH 7.5, 1 mM sodium benzoate, 1 mM DTT, 5% glycerol) and allowed to incubate for 1 h with occasional stirring. After removal of the supernatant, the resin was poured into a column, washed with 1 L of buffer A + 100 mM NaCl, and eluted with buffer A + 300 mM NaCl. The protein was pooled and diluted with buffer A to lower the conductivity to less than that of buffer A + 100 mM NaCl, and the solution was applied to a second DEAE-Sepharose Fast Flow column (500 mL, 4.8 × 27 cm) equilibrated in buffer A. The column was washed with 1 L of buffer A + 100 mM NaCl followed by application of a 5 L linear gradient from 100 to 400 mM NaCl in buffer A (2 mL/min). Fractions containing at least 20% of the maximum enzyme activity were pooled. This step separated the two components of BZDOS.

The DEAE pool of oxygenase was concentrated in an Amicon stirred ultrafiltration cell using a YM-100 membrane. Concentrated BZDO was applied to a 2.2 L (4.8 × 120 cm) Ultrogel AcA 34 (Sepracor) or Sephacryl S300 (Sigma) size-exclusion column equilibrated in buffer A and developed with buffer A at 0.5 mL/min. Fractions containing 20% or more of the maximum enzyme activity were pooled. BZDO was concentrated as above, and aliquots were immediately frozen in liquid nitrogen and stored at −80 °C. Enzyme purified in this manner, termed $BZDO_I$, contained ~2.7 Fe/$\alpha\beta$[2] with the mononuclear iron in the ferric state (see Results).

BZDO Purification (Method II). A second purification method was used to produce a highly active BZDOS preparation that did not contain benzoate. All of the chromatography steps described for method I were utilized with the following modifications: all buffers were bubbled with N_2 prior to use to decrease the dissolved O_2 concentration, benzoate was omitted from the buffers, and the size-exclusion column was equilibrated and developed in 100 mM MOPS buffer, pH 6.9, 1 mM DTT, and 5% glycerol. This preparation of BZDO ($BZDO_{II}$) typically contained about 2.6 Fe/$\alpha\beta$ and exhibited the same specific activity as $BZDO_I$, but the mononuclear iron was in the ferrous state (see below).

BZDR Purification. Pooled BZDR from the second DEAE-Sepharose column was concentrated in an Amicon ultrafiltration cell using a YM-30 membrane, loaded onto a 490 mL (2.5 × 100 cm) Ultrogel AcA 44 (Sepracor) size-exclusion column equilibrated in buffer A + 100 mM NaCl, and developed in the same buffer at 0.5 mL/min. Fractions containing 20% or more of the maximum enzyme activity were pooled. The pooled fractions were loaded onto a 120 mL (2.6 × 23 cm) DEAE-Sepharose Fast Flow column equilibrated in buffer B (25 mM MOPS, pH 6.5, 1 mM DTT, 5% glycerol). The column was washed with two volumes of buffer B + 150 mM NaCl, and BZDR was eluted by running a 1 L linear gradient from 150 to 500 mM NaCl in buffer B (1 mL/min). Fractions containing 20% or more of the maximum activity were pooled, concentrated, and stored as described for BZDO.

Partial Purification of 1,2-CTD. 1,2-CTD was pooled as it eluted from the second DEAE-Sepharose column immediately before BZDR. 1,2-CTD activity was assayed polarographically at 23 °C by monitoring O_2 consumption in air-saturated 50 mM MOPS, pH 6.9, with a Clark-type electrode as described previously (*16*). Fractions containing greater than 10% maximum activity were pooled, dialyzed against 50 mM Tris−acetate, pH 8.5 (3 × 2 L), and stored at 4 °C.

Partial Purification of Benzoate cis-Diol Dehydrogenase (CDD). The second enzyme in the benzoate degradation pathway is the NAD^+-dependent dehydrogenase that catalyzes the decarboxylation and rearomatization of benzoate *cis*-diol to catechol (*17*, *18*). The enzyme was pooled from the second DEAE-Sepharose column where it eluted before BZDR. The CDD pool was concentrated using a Centricon 10 ultrafiltration device and applied to a 100 mL AcA 44 size-exclusion column equilibrated and developed in 50 mM Tris buffer, pH 7.8, and 5% glycerol. The CDD-containing fractions were pooled, concentrated, and stored at −80 °C. The size-exclusion step was required to remove an unknown contaminating protein that had NADH-dependent oxidase activity that interfered with assays. CDD activity was measured by monitoring the increase in absorption of NADH ($\epsilon_{340} = 6.23\ mM^{-1}\ cm^{-1}$) using authentic benzoate *cis*-diol as the substrate.

BZDOS Assays. BZDO activity was determined polarographically at ambient temperature (23−24 °C) in a standard reaction mixture containing 100 mM MOPS, pH 6.9, 0.1 M NaCl, 1.0 mM sodium benzoate, 0.3 mM NADH, and 1 μM BZDR. The large amounts of BZDR required for maximal oxygenase activity prohibit routine analysis under saturating conditions. Minor background rates of uncoupled O_2 consumption by NADH and BZDR were subtracted from the total consumption rate. Reactions with substituted benzoates contained 10 mM substrate, 50 μM NADH, 1.8 μM BZDR, and 0.7 μM BZDO. Eighty units of bovine catalase was

[2] Because BZDO consists of three ($\alpha\beta$) dimers with each heterodimer containing one active site, all stoichiometries and activities of BZDO or BZDOS are referenced to a single $\alpha\beta$ active site.

added when oxygen consumption ceased to assess the amount of uncoupled turnover, which yields hydrogen peroxide as a product. One unit of oxygenase activity is defined as the amount of enzyme required to consume 1 μmol of O_2 in 1 min.

BZDR was routinely assayed at 23 °C by following the reduction of $K_3Fe(CN)_6$ spectrophotometrically at 420 nm ($\epsilon_{420} = 1.02$ mM^{-1} cm^{-1}). The assay mixture contained 50 mM HEPES, pH 8.0, 1 mM $K_3Fe(CN)_6$, and 0.3 mM NADH in 1 mL. The assay was initiated by the addition of reductase. Rates were calculated from initial velocities after subtraction of background rates of $K_3Fe(CN)_6$ reduction by NADH. One unit of activity is defined as the amount of reductase that catalyzes the reduction of 1 μmol of $K_3Fe(CN)_6$ in 1 min.

Preparation of Mononuclear Iron-Depleted BZDO. Mononuclear iron was removed from BZDO by dialyzing the concentrated enzyme against chelators. $BZDO_I$ was placed into a Slide-A-Lyzer cassette (Pierce) and dialyzed against four changes of a 100× volume of 50 mM HEPES, pH 7.5, 5% glycerol, and 10 mM EDTA over 24 h with stirring at 4 °C. $BZDO_{II}$ was dialyzed against the same buffer with the addition of 1 mM *o*-phenanthroline. The chelators were removed by a single 2 h dialysis (100× volume) against 50 mM MOPS, pH 6.9, 1 mM DTT, and 5% glycerol, followed by application of the enzyme to a 120 mL Sephadex G-25 (Pharmacia) column equilibrated in the same buffer. The enzyme ($BZDO_{apo}$) was concentrated and stored as described above. $BZDO_{apo}$ typically contained 1.9 Fe/$\alpha\beta$ from the Rieske cluster.

Reconstitution of $BZDO_{apo}$. Iron reconstitutions of mononuclear iron-depleted $BZDO_{apo}$ were completed on ice under anaerobic conditions. Stock solutions of Fe(II) were made from $Fe(NH_4)_2(SO_4)_2 \cdot 6H_2O$ buffered with 100 mM MOPS, pH 6.9. $BZDO_{apo}$ (0.5−1.0 mM $\alpha\beta$) was incubated with 5 mM Fe(II) for 1 h and then applied to a 50 mL Sephadex G-25 column equilibrated in Ar-purged 50 mM MOPS buffer, pH 6.9, 1 mM DTT, and 5% glycerol. Brown fractions of the reconstituted enzyme ($BZDO_{rec}$) were collected, pooled, concentrated, and stored at −80 °C. Attempts to reconstitute $BZDO_{apo}$ with Fe(III) were also performed using a stock solution of $FeCl_3 \cdot 6H_2O$ following the same procedure described for Fe(II). The extent of reconstitution was evaluated by iron content, EPR spectroscopy, and enzyme activity. While reconstitution with Fe(III) was unsuccessful, the reconstitution of $BZDO_{apo}$ with Fe(II) typically yielded enzyme with 2.5 Fe/$\alpha\beta$.

^{57}Fe Incorporation. The mononuclear iron site of BZDO was enriched with ^{57}Fe by reconstituting $BZDO_{apo}$ containing unenriched Rieske cluster with ^{57}Fe(II) prepared from ^{57}Fe metal under anaerobic conditions. The iron foil was first dissolved in a degassed solution of concentrated H_2SO_4 (3 mol equiv) and concentrated H_2NO_3 (1 mol equiv). The iron solution was diluted to 50−200 mM Fe with 1 M MOPS, pH 6.9, and 20 mM DTT. Aliquots of the ^{57}Fe solution were added to the $BZDO_{apo}$ solution to a concentration of 5 mM, and the remaining steps of the reconstitution were performed as described above. Enrichment of the Rieske cluster with ^{57}Fe was completed by growing *P. putida* mt-2 in minimal media as described above with the following modification: all precursor solutions used in MSB−benzoate were made without addition of the prescribed iron, and ^{57}Fe was added from a stock solution to a final concentration similar to the iron concentration in MSB−benzoate. Other procedures were as described for method I. Because this procedure enriched both the Rieske and mononuclear iron sites, the mononuclear ^{57}Fe was removed and replaced with ^{56}Fe by the standard reconstitution procedure.

Protein Purity, Molecular Weight, and Composition. The protein purity and molecular weight were analyzed by SDS−PAGE under denaturing conditions. Analytical ultracentrifugation was performed as previously described (*19*). Flavin content of BZDR was determined by treating the enzyme with 3 N HCl followed by centrifugation to remove precipitated protein. The flavin was identified as FAD by comparison of its optical spectrum to those of both FMN and FAD, as well as by thin-layer chromatography [mobile phase: 1-butanol/acetic acid/H_2O (4/2/3); $FMN_{Rf} = 0.66$, $FAD_{Rf} = 0.46$, $BZDR_{Rf} = 0.47$]. FAD content was quantified by UV/vis spectroscopy ($\epsilon_{450} = 11300$ M^{-1} cm^{-1}). The metal to protein stoichiometry was determined by inductively coupled plasma emission spectroscopy (University of Minnesota Soil Sciences Department) and amino acid analysis (University of Minnesota Microchemical Facility) performed on the same sample. Routine measurements of iron content were made by either atomic absorption (Varian SpectAA 100) or the method of Fish (*20*). Mononuclear iron content was determined as described previously (*7*). The extinction coefficients for BZDOS components were found to be nearly identical to those reported for BZDOS isolated from *P. putida* C-1 (*11*−*13*). BZDR: $\epsilon_{273} = 62$ mM^{-1} cm^{-1}; $\epsilon_{467} = 21$ mM^{-1} cm^{-1}. BZDO: $\epsilon_{280} = 133$ mM^{-1} $\alpha\beta^{-1}$ cm^{-1}; $\epsilon_{325} = 15$ mM^{-1} $\alpha\beta^{-1}$ cm^{-1}; $\epsilon_{464} = 7.8$ mM^{-1} $\alpha\beta^{-1}$ cm^{-1}.

Anaerobic Technique, Preparation of Nitrosyl Complexes, and Protein Reduction. Anaerobiosis was attained, and nitrosyl complexes were prepared using methods previously described (*7*). Protein reduction was completed under anaerobic conditions by addition of aliquots of a buffered dithionite stock solution in the presence of methyl viologen (20 μM for EPR measurements, 100 μM for all other experiments) until a faint blue color from reduced methyl viologen was detected, indicating that the enzyme was stoichiometrically reduced.

Spectroscopy. Electronic absorption spectra were recorded using a Hewlett-Packard 8453 diode array spectrophotometer. EPR spectra were recorded using a Bruker E-500 spectrometer and an Oxford 910 liquid helium cryostat and were analyzed as previously described (*7*). *E*/*D* was determined from the *g*-values as previously described (*7*). The EPR spectra of Figure 9 were recorded on a Bruker 300 spectrometer equipped with an Oxford ESR 910 cryostat for low-temperature studies. The Oxford thermocouple temperature was calibrated using a carbon−glass resistor probe (CGR-1, Lake Shore Cryotronics). For determination of the spin concentrations the system was calibrated against CuEDTA for which the copper concentration was determined by plasma emission spectroscopy. The spectra were analyzed using a software package written by Dr. M. P. Hendrich at Carnegie Mellon University. The microwave power required for half-saturation ($P_{1/2}$ value) of the nitrosyl complexes was determined by measuring the intensity of the low-field EPR resonance ($g = 4.1$−4.2) at different powers and fitting the data to the equation:

$$S' = (I/\sqrt{P})/(I_0/\sqrt{P_0}) = (1 + P/P_{1/2})^{-b/2} \qquad (1)$$

Table 2: Comparison of Physical Properties of Two- and Three-Component Rieske Dioxygenases

	benzoate 1,2-dioxygenase[a] (*P. putida* mt-2)	benzoate 1,2-dioxygenase[b] (*P. putida* C-1)	phthalate dioxygenase[c] (*B. cepacia*)	naphthalene 1,2-dioxygenase[d] (*P.* sp. NCIB)
oxygenase component				
subunit structure	$(\alpha\beta)_3$	$(\alpha\beta)_3$	α_4	$(\alpha\beta)_3$
subunit MW (kDa)	$\alpha = 49$ $\beta = 19$	$\alpha = 50$ $\beta = 20$	$\alpha = 48$	$\alpha = 55$ $\beta = 20$
molecular mass (kDa)				
sedimentation analysis	195	201	*e*	210
SDS−PAGE	204	210	192	225
Fe content (mol/mol of $\alpha\beta$)	2.7	2.7	2.7	2.7
specific activity (units/mg)[f]	24	19.7	18.4	26
ferredoxin component	none	none	none	14 kDa[g]
reductase component				
molecular mass (kDa)				
sedimentation analysis		38.3		
SDS−PAGE	38	37.5	34.4	36.0
flavin content	0.96	1.0	1.0	0.15
Fe content	2.02	2.08	1.91	2.0
specific activity (units/mg)[h]	790	697	120	1225[i]

[a] This work. [b] Data from refs *11*−*13*. [c] Data from ref *8*. [d] Data from refs *7* and *21*−*23*. [e] A molecular mass of 217 kDa was determined by gel filtration chromatography and is used as the holoenzyme mass. [f] Determined at ambient temperature (23−25 °C) under conditions of saturating components. In the case of BZDOS from *P. putida* mt-2, the K_M for BZDR ranges from 5 to 10 μM and depends on the ionic strength. Steady-state activity is maximized at ∼100 mM NaCl at pH 6.9. Using the standard assay with 1 μM BZDR, the specific activity is 1.5−2.0 units/mg, which increases to ∼2.6 units/mg upon saturation with added Fe(II). [g] The NDOS ferredoxin component contains one Rieske-type [2Fe-2S] cluster. [h] Activity determined with $K_3Fe(CN)_6$ as electron acceptor. [i] Supplemented with 1 nmol of FAD.

where S' is the normalized signal intensity, I is the signal intensity measured at a temperature of 4 K, P is the microwave power, and b is a parameter describing the broadening mechanism.

The Mössbauer spectrometer was of the constant acceleration type equipped with a Janis Supervaritemp cryostat. Isomer shifts are reported relative to iron metal at room temperature.

Single Turnover Reactions and Product Analysis. Single turnover reactions to determine product yield were carried out in 100 mM MOPS, pH 6.9, using stirred, septum-sealed reaction vials. BZDO (50 nmol of BZDO active sites) was first made anaerobic and stoichiometrically reduced with dithionite in the presence of 100 μM methyl viologen in a total volume of 500 μL. Turnover was initiated at 23 °C by addition of an equal volume of O_2-saturated buffer (∼1.2 mM at 23 °C) containing 2 mM sodium benzoate. Where indicated, 50 nmol of BZDR was included in the reaction, or $Fe(NH_4)_2(SO_4)_2 \cdot 6H_2O$ was added to a final concentration of 100 μM. Reactions were transferred to Eppendorf tubes and terminated at 1 min by immersion into a 90 °C water bath for 2 min, resulting in the total loss of activity. Longer reaction times did not result in increased yield of product. Samples were briefly vortexed and frozen in liquid N_2 until product analysis was performed. No breakdown of authentic benzoate *cis*-diol is observed during this treatment. Because of the instability of the product under HPLC conditions, production of benzoate *cis*-diol was measured by coupling benzoate *cis*-diol production to NADH formation using the NAD^+-dependent CDD. Samples for assay were thawed and centrifuged for 2 min at 20000*g* to pellet precipitated protein, and the supernatant was transferred to a cuvette to which the CDD (0.18 unit) and NAD^+ (1 mM) were added. The reaction was monitored at 340 nm for NADH formation until no further increase in absorption was observed (about 3 min). For precision, a standard curve using authentic benzoate *cis*-diol was generated under identical conditions and used for the determination of product formed during the single turnover reaction.

Spectroscopic Analysis of Single Turnover Reactions. Single turnover reactions to be monitored by EPR spectroscopy were performed in septum-sealed, stirred reaction vials containing 200 μM BZDO sites in 100 mM MOPS, pH 6.9, at 23 °C. The enzyme was reduced stoichiometrically with dithionite and 20 μM methyl viologen and mixed with either an equal volume of anaerobic buffer or an equal volume of oxygenated buffer each containing 10 mM benzoate. The mixture was then rapidly transferred (within 10 s) to EPR tubes and frozen in liquid N_2 after 60 s. Stopped-flow reactions were performed at 4 °C using an Applied Photophysics model SX.18MV stopped-flow instrument with the following reactants: syringe 1 contained anaerobic 60 or 100 μM stoichiometrically reduced BZDO in 50 mM MOPS, pH 6.9; syringe 2 contained 2 mM benzoate in O_2-saturated (1.8 mM) 50 mM MOPS, pH 6.9. Single turnover samples for Mössbauer spectroscopy were prepared at 23 °C as follows: BZDO (1 mM $\alpha\beta$), benzoate (10 mM), and methyl viologen (100 μM) were mixed and made anaerobic, and the enzyme was stoichiometrically reduced with dithionite in a septum-sealed reaction vial. An aliquot was transferred to a Mössbauer cup using a Hamilton gastight syringe. The cup was contained within a septum-sealed vial maintained under 1 atm of Ar. The sample in the cup was frozen in liquid N_2 while still in the anaerobic vial. The remaining enzyme mixture was reacted with oxygen by vigorously flushing the surface of the solution with O_2 for 20 s. The sample was transferred to a Mössbauer cup and frozen in liquid N_2.

RESULTS

Stabilization, Purification, and Properties of P. putida mt-2 BZDOS. A common problem with Rieske dioxygenase preparations is the isolation of inactive protein due to loss of mononuclear iron from the oxygenase component. We have found that addition of substrate to (preparation $BZDO_I$), or removal of O_2 from (preparation $BZDO_{II}$), the BZDOS purification buffer stabilizes the mononuclear iron center of the BZDO component, reducing the loss of activity. Through application of these approaches, the two components of the

Table 3: Optical and EPR Spectroscopic Properties of *P. putida* mt-2 Benzoate 1,2-Dioxygenase

protein component	UV/vis λ_{max} [ϵ (mM^{-1} cm^{-1})]	EPR parameter	
		g-value	*E/D*
$BZDO_I$			
[2Fe-2S]	325 (15), 464 (7.8)		
mononuclear Fe	no[a]	7.6, 4.2, 1.83	0.076
		4.3	0.33
$BZDO_{II}$			
[2Fe-2S]	325 (15), 464 (7.8)		
mononuclear Fe	no		
reduced BZDO			
[2Fe-2S]	380 (5.9), 520 (2.9)	2.01, 1.91, 1.77	
mononuclear Fe	no		
BZDO after turnover			
[2Fe-2S]	325 (15), 464 (7.8)[b]	*b*	
mononuclear Fe	no	8.25, 3.35, 1.63[c]	0.115
		4.3	0.33
$BZDO_{II} + O_2$			
mononuclear Fe	no	7.6, 4.2, 1.83	0.076
$BZDO_{II}$ + benzoate + O_2			
mononuclear Fe	no	4.3	0.33
$BZDO_{II}$ + *cis*-diol + O_2			
mononuclear Fe	no	8.25, 3.35, 1.63	0.115
		4.3	0.33
oxidized BZDR			
[2Fe-2S], FAD	345 (17), 467 (21)		
$2e^-$ reduced BZDR			
[2Fe-2S], $FADH^\bullet$	467 (9.8), 640[d] (1.9)	2.05, 1.95, 1.88; 2.006[d]	
$3e^-$ reduced BZDR			
[2Fe-2S], $FADH_2$	467 (5.1), 540 (3.4)	2.05, 1.95, 1.88	

[a] Not observed. Comparison of the spectrum with that of $BZDO_{apo}$ shows no apparent charge-transfer band from the mononuclear iron. [b] Greater than 1 h is required to fully oxidize the Rieske cluster. [c] The $g = 1.63$ feature has not been observed. The position of this feature depends strongly on *E/D*, and the resonance broadens significantly when *E/D* is distributed. The same considerations apply for the $g = 1.83$ feature of the *E/D* 0.076 species. [d] The absorption at 640 nm and EPR resonance at $g = 2.006$ represent the neutral blue flavin semiquinone of reduced BZDR.

benzoate 1,2-dioxygenase system from *P. putida* mt-2 were purified to homogeneity using standard chromatographic techniques as summarized in Table 1 (see Materials and Methods). The two different methods used to stabilize BZDO during purification resulted in enzymes with identical physical parameters except for the oxidation state of the mononuclear iron (see below). Table 2 shows that the physical properties of the *P. putida* mt-2 enzyme are very similar to those of the BZDOS isolated previously from *P. putida* C-1. A relatively broad range of substituted benzoates serves as alternative substrates for the two enzymes with only minor differences in relative turnover rates (for a list see ref *12*). The general properties of the BZDOS enzymes are similar to those of Rieske dioxygenases from other subclasses (Table 2), although differences in the number of electron transfer chain components and the oxygenase component subunit properties and quaternary structure that form the basis for the classification system are apparent.

Importance of the Mononuclear Iron Site. As observed for other Rieske dioxygenases, removal of the mononuclear iron from $BZDO_I$ or $BZDO_{II}$ while leaving the Rieske cluster intact ($BZDO_{apo}$) led to >90% loss of activity. The remaining activity probably reflects residual iron in the assay mixture, oxidase activity of $BZDO_{apo}$, or both. Full activity of the enzyme as isolated was recovered by adding Fe(II) to the $BZDO_{apo}$ assay. In a separate experiment, $BZDO_{apo}$ was reconstituted with Fe(II) in the absence of assay components to yield $BZDO_{rec}$ (see Materials and Methods). $BZDO_{rec}$ has catalytic properties nearly identical with those of $BZDO_{II}$ as isolated, consistent with ~2.5 total iron per $\alpha\beta$ and ~0.6 mononuclear Fe/$\alpha\beta$. $BZDO_{apo}$ failed to bind Fe(III) under identical reconstitution conditions.

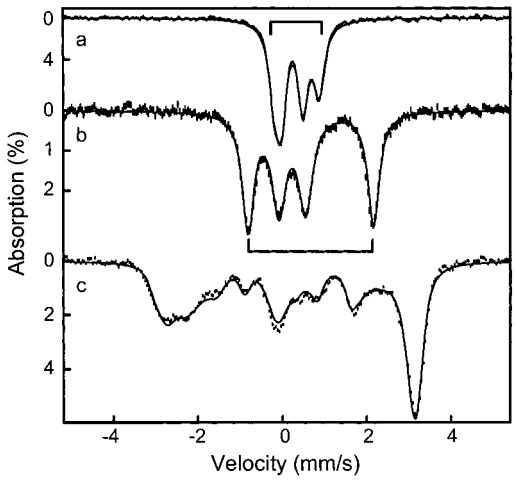

FIGURE 1: Mössbauer spectra of the [2Fe-2S] Rieske-type cluster of BZDO. Shown are spectra of $BZDO_{rec}$ (2.1 mM sites) with ^{57}Fe incorporated only into the Rieske cluster as described in Materials and Methods. (a) Spectrum of the oxidized cluster recorded in zero field at 4.2 K. The solid line is a fit to two quadrupole doublets using the parameters quoted in Table 4. (b) Spectrum of the reduced cluster recorded at 195 K in zero field. The solid line is a fit to two doublets of equal intensity. The brackets in (a) and (b) designate the doublets assigned to the FeS_2His_2 site of the Rieske cluster. (c) 4.2 K spectrum of the reduced cluster recorded in a 0.5 T field applied parallel to the observed γ-radiation. The fit is a spectral simulation using the parameter set listed in Table 4. (For details see ref *24*.)

In the following sections describing spectroscopic and kinetic results, it is useful to keep in mind that $BZDO_I$ was prepared in the presence of benzoate and that benzoate is in the buffer for all experiments unless stated otherwise. In contrast, no benzoate was present for experiments involving $BZDO_{II}$, $BZDO_{apo}$, or $BZDO_{rec}$, unless it is specifically stated that it was added.

Spectroscopic Properties. The optical spectra of the BZDOS components are consistent with those of other members of the Rieske dioxygenase family and are summarized in Table 3. As isolated, $BZDO_I$ and $BZDO_{II}$ have electronic absorption maxima at 325 and 464 nm (ϵ_{464} = 7800 M^{-1} cm^{-1}), indicating that the Rieske cluster is oxidized. Bleaching of the visible spectrum occurs upon addition of dithionite or NADH and catalytic amounts of BZDR, and this change can be used to monitor electron transfer to and from the cluster (see below).

Figure 1 shows Mössbauer spectra of the oxidized and reduced Rieske cluster of BZDO. The 4.2 K spectrum of Figure 1a exhibits two doublets with $\Delta E_Q(1) = 0.51$ mm/s, $\delta(1) = 0.24$ mm/s and $\Delta E_Q(2) = 1.05$ mm/s, $\delta(2) = 0.35$ mm/s. These parameters are nearly the same as those reported for the Rieske clusters of the toluene-4-monooxygenase system from *Pseudomonas mendocina* (*24*) and the ferredoxin from *Thermus thermophilus* (*25*). The two doublets represent the inequivalent iron sites of the $S = 0$ state of the

Table 4: 4 K Mössbauer Parameters of Benzoate 1,2-Dioxygenase

sample	spin		δ^a (mm/s)	ΔE_Q (mm/s)	η	A_x (MHz)	A_y (MHz)	A_z (MHz)	% Fe
BZDR (ox)	0	site 1	0.27	0.55					50
		site 2	0.28	0.86					50
BZDR (red)[b]	$^1/_2$	ferric	0.30	0.8	0	−55	−49	−44	50
		ferrous	0.65	−3.0	−1	+11	+25	+36	50
Rieske (ox)	0	site 1	0.24	0.51					50
		site 2	0.35	1.05					50
Rieske (red)	$^1/_2$	ferric	0.30	0.65	0	−55	−48	−44	50
		ferrous	0.75	−3.2	−2[c]	+13	+14	+30	50
mono Fe(II)	2	site I	1.26	3.1					75 (3)
		site II	1.27	2.0					25 (3)
mono Fe(III) after turnover[d]	$^5/_2$		≈0.45	≈1.0	0.5	−26.7	−26.7	−26.7	50 (10)

[a] Isomer shifts are quoted at 4.2 K relative to Fe metal at 298 K. [b] This state has *g*-values at 1.88, 1.95, and 2.05. [c] The largest component of the electric field gradient tensor is positive and directed along the *x*-axis. In a proper coordinate system of the field gradient tensor $\Delta E_Q > 0$ and $\eta = 0.33$. [d] $D = 3.0\ cm^{-1}$ and $E/D = 0.115$.

oxidized cluster. Upon reduction by dithionite, the Rieske cluster assumes the exchange-coupled $S = {}^1/_2$ state. The spectrum of Figure 1b was recorded at 195 K under conditions where the electronic spin relaxes fast compared to the nuclear precession frequencies, and therefore, only quadrupole doublets are observed. The spectrum exhibits a doublet representing a high-spin ferric site with $\Delta E_Q(1) = 0.65$ mm/s and $\delta(1) = 0.23$ mm/s and a doublet of a high-spin ferrous site with $\Delta E_Q(2) = 2.99$ mm/s and $\delta(2) = 0.68$ mm/s; by correcting for the temperature-dependent second-order Doppler shift, we obtain the isomer shifts at 4.2 K, $\delta(1) = 0.30$ mm/s and $\delta(2) = 0.75$ mm/s. Comparison of the δ-values of the two sites in the two oxidation states shows that site 2 is the site coordinated by the two histidyl residues, and it is this site that accommodates the electron that enters the cluster upon reduction (in Figure 1 the doublets of site 2 are marked by the brackets). The low-temperature spectra of the Rieske cluster, shown in Figure 1c, are very similar to those observed for the *P. mendocina* Rieske protein and were fit in the same way (*24*) to give the parameters listed in Table 4. During this study, we have also recorded Mössbauer spectra of the [2Fe-2S] cluster of BZDR (not shown); for completeness, we have included its parameters in Table 4.

Figure 2a shows a 4.2 K Mössbauer spectrum of BZDO with ^{57}Fe enrichment at the mononuclear center (see Materials and Methods). The spectrum shown consists of a superposition of (essentially) two doublets. Doublet I, representing ca. 75% of the Fe, has $\Delta E_Q = 3.1$ mm/s and $\delta = 1.26$ mm/s while doublet II (bracket) exhibits $\Delta E_Q = 2.0$ mm/s and $\delta = 1.27$ mm/s. Both doublets represent high-spin ferrous ions. We have observed similar spectra for other preparations, with some variability in the amount of Fe represented by each doublet. Strictly speaking, doublet II represents a distribution of species with ΔE_Q values centered about the mean value of 2.0 mm/s. We have represented this distribution by assuming absorption lines with Voigt shapes (using a convolution of a Lorentzian with 0.15 mm/s width into a Gaussian having width $\sigma = 0.4$ mm/s). In the absence of substrate, essentially the same doublets were observed, albeit with slightly different intensity ratios. These data indicate that the reconstituted oxygenase contains mononuclear iron in at least two different electronic environments, which appear to be sensitive to substrate binding. We also observe two species using EPR spectroscopy as described below.

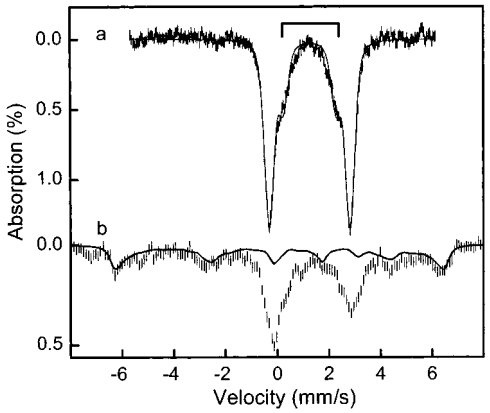

FIGURE 2: 4.2 K Mössbauer spectra of the ^{57}Fe-enriched BZDO mononuclear iron center. (a) Spectrum of the ferrous site (≈400 μM ^{57}Fe) recorded in zero field. The spectrum contains two major species with $\Delta E_Q = 3.1$ mm/s (75% of ^{57}Fe) and $\Delta E_Q = 2.0$ mm/s (25%). The solid line is a spectral simulation for these doublets using Voigt lines with 0.4 mm/s Gaussian width to account for the relatively broad lines. (b) Spectrum of BZDO following single turnover. The sample (ca. 300 μM ^{57}Fe) was reduced stoichiometrically with dithionite and methyl viologen and then made 10 mM in benzoate. Finally, it was exposed to O_2 for 20 s as described in Materials and Methods. The spectrum was collected at 4.2 K with a 0.05 mT magnetic field applied parallel to the incident γ-radiation. The solid line, scaled to correspond to 50% of total ^{57}Fe, is a fit to an $S = {}^5/_2$ species with $D = 3.0\ cm^{-1}$ and $E/D = 0.115$ (ca. 50% of total absorption) using the parameters listed in Table 4.

The EPR spectra of high-spin ferric ions are commonly described with the $S = {}^5/_2$ spin Hamiltonian:

$$H = D[\mathbf{S}_z^2 - S(S+1)/3] + E(\mathbf{S}_x^2 - \mathbf{S}_y^2) + 2.00\beta\mathbf{S}\cdot\mathbf{B} \quad (2)$$

D and E are the axial and rhombic zero-field splitting parameters, respectively. The zero-field splitting term removes the 6-fold degeneracy of the spin sextet, and three Kramers doublets result. For $|D| \gg \beta B$ it is convenient to describe the magnetic properties of each doublet by effective *g*-values; all values quoted below are effective *g*-values. These *g*-values depend only on the parameter E/D; the energy of the three doublets depends on D and E/D. Table 3 summarizes the EPR properties of both components of BZDOS.

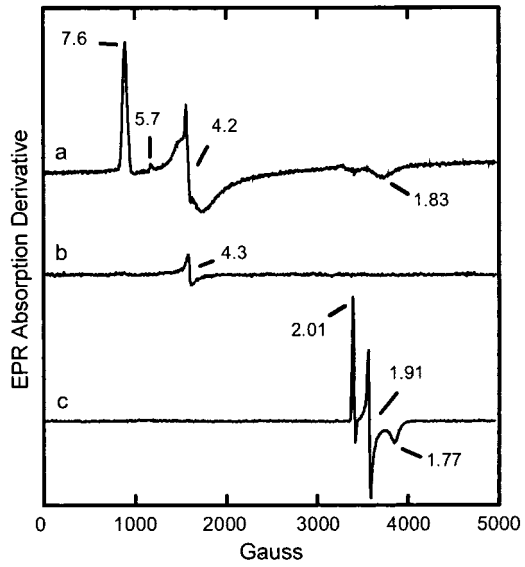

FIGURE 3: EPR spectra of BZDO purified by methods I and II. Samples contained 450 μM BZDO sites: (a) $BZDO_I$, (b) $BZDO_{II}$, and (c) $BZDO_{II}$ reduced with dithionite plus 20 μM methyl viologen. The sharp dip below the baseline near the $g = 2.01$ resonance in (c) results from the reduced methyl viologen radical. Instrument conditions: microwave power, 100 μW (a, b) and 200 μW (c); temperature, 2 K (a, b) and 25 K (c); modulation amplitude, 10 G; microwave frequency, 9.63 GHz.

The EPR spectrum of $BZDO_I$ shown in Figure 3a reveals two $S = {}^5/_2$ species with different E/D values. The major species has $E/D = 0.076$ ($g_x = 4.2$, $g_y = 7.6$, and $g_z = 1.83$ result from the ground doublet, roughly the $M_s = \pm{}^1/_2$ state, and $g_z = 5.7$ belongs to the middle doublet). Temperature-dependent changes in intensity of the $g = 7.6$ and 5.7 features were used to establish $D = +1.3$ cm^{-1} for this species. The minority species has a rhombic $E/D = 0.33$, yielding the isotropic $g = 4.3$ resonance originating from the middle Kramers doublet of this species. After subtraction of the small signal from the rhombic species, the more axial $E/D = 0.076$ Fe(III) content was estimated to be 0.6−0.9 spin/$\alpha\beta$ depending on the particular batch of enzyme analyzed.

Figure 3b shows the EPR spectrum of $BZDO_{II}$. No evidence for significant concentrations of mononuclear Fe(III) in either the high- or low-spin states is observed, suggesting that the mononuclear iron present in the sample is ferrous (see below). As isolated, neither $BZDO_I$ nor $BZDO_{II}$ shows anisotropic EPR signals near $g = 2$, indicating that the Rieske cluster is in the oxidized, diferric $[2Fe\text{-}2S]^{2+}$ state. Figure 3c shows the spectrum of $BZDO_{II}$ after addition of excess dithionite. Resonances at $g = 2.01$, 1.91, 1.77 ($g_{av} = 1.89$) result from antiferromagnetic coupling of the ferric and ferrous ions of the reduced Rieske cluster. An identical spectrum is observed for reduced $BZDO_I$. Integration of the signal yields 0.8−1.0 spin/$\alpha\beta$, varying with different batches of enzyme. Since reduced $BZDO_I$ and $BZDO_{II}$ have identical spectra, the presence of benzoate in the $BZDO_I$ preparation apparently does not alter the electronic environment of the Rieske cluster.

Substrate Complexes of BZDO as Isolated. The mononuclear iron of Rieske dioxygenases is proposed to be the site of both O_2 and substrate binding. The EPR spectra shown in Figure 4a−c indicate that only the minor rhombic species at $g = 4.3$ is affected by the removal and subsequent addition

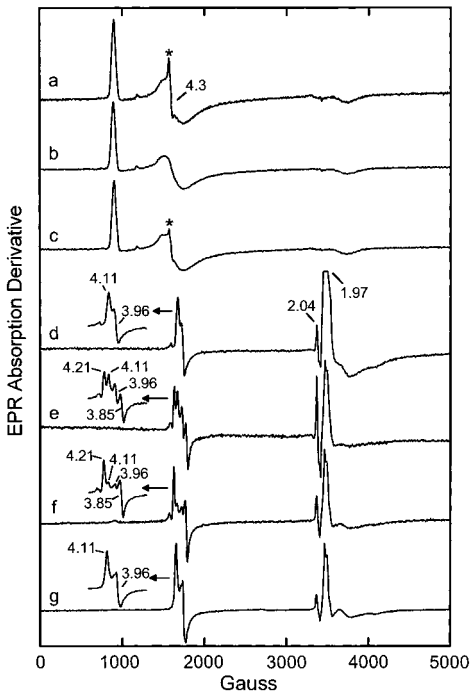

FIGURE 4: EPR spectra showing effects of substrate binding to BZDO. Spectra a−c show EPR spectra of $BZDO_I$ (500 μM sites) (a) as isolated in the presence of benzoate, (b) following removal of benzoate by gel filtration, and (c) after addition of 10 mM benzoate to (b). The asterisk (✱) marks the sharp signal from Fe(III) with maximal rhombic symmetry that is present only in samples containing benzoate. Benzoate binding to BZDO with ferrous mononuclear ion is demonstrated in spectra d−g. The normally EPR-silent $BZDO_{II}$ (450 μM sites) was made EPR active by exposure to NO in the absence (d) or presence (e) of 10 mM benzoate. (f) Spectrum of $BZDO_I$ (500 μM sites) after exposure to NO, which causes the reduction of the mononuclear iron by an unknown mechanism. (g) Spectrum of $BZDO_I$ after removal of the benzoate and exposure to NO. Insets: Expanded views of the $g = 4$ region of the nitrosyl complexes (not aligned with the magnetic field axis of the main figure). The origins of the anomalous signals near $g = 2$ are described in the text. Instrument conditions: (a−c) microwave power, 100 μW; temperature, 2 K; modulation amplitude, 10 G; microwave frequency, 9.63 GHz; (d−g) the same except microwave power, 200 μW, and temperature, 10 K.

of benzoate to $BZDO_I$. Because this species represents only a few percent of the total Fe(III) content of the enzyme, it is unlikely that the changes reflect an alteration in the entire population of mononuclear iron sites in the sample. One possibility is that the two different types of iron centers reflect two different ways that benzoate can bind in the active site. Another possibility is that despite its presence in solution, benzoate cannot gain access to the majority of the mononuclear iron sites so that the $E/D = 0.076$ center is the substrate-free form of BZDO. Support for this latter possibility is reported below. If this is the case, then the $E/D = 0.33$ species represents the true substrate complex.

While the EPR data for $BZDO_I$ seem to indicate that substrate in solution does not affect the environment of the majority Fe(III) mononuclear iron site, it can readily be shown that this is not the case for the mononuclear Fe(II) centers of $BZDO_{II}$ and reduced $BZDO_I$. The mononuclear Fe(II) site of $BZDO_{II}$ is EPR silent at X-band, but upon exposure to nitric oxide, an axial $S = {}^3/_2$ complex forms with effective g-values $g_y = 4.11$, $g_x = 3.96$, and $g_z = 2.0$ (line width at g_y, $g_x = 40$ G, $E/D = 0.012$) (Figure 4d). We

have shown this spectrum to be characteristic of an Fe(II)−nitrosyl complex in several other mononuclear iron-containing enzymes (see, for example, refs *26* and *27*). Integration of the $BZDO_{II}$−NO spectrum yielded ~0.6 spin/$\alpha\beta$ but exhibited the same batch-to-batch variability described above. Two other signals observed at $g \approx 2$ result from NO interacting with the Rieske cluster ($g = 2.04$, <0.05 spin/$\alpha\beta$) and dissolved NO ($g = 1.97$).[3] As shown in Figure 4e, addition of 10 mM benzoate to the NO complex causes two major changes in the EPR spectrum, suggesting that benzoate binds near the mononuclear iron. First, a sharp $S = {}^3/_2$ species ($g_y = 4.21$, $g_x = 3.85$, and $g_z = 2.0$; line width at g_y, g_x = 25 G) forms that is more rhombic ($E/D = 0.029$) than that of the binary Fe(II)−NO complex. Second, upon addition of benzoate, the $E/D = 0.012$ species decreases in intensity, and its line width sharpens to 25 G. Spectral simulation indicates that the $E/D = 0.029$ and $E/D = 0.012$ species are formed in about a 2:1 ratio. Integration of all NO complexes yielded the same number of spins as originally present in the binary complex, suggesting that the $E/D = 0.029$ species was formed from the binary complex. As expected, $BZDO_{apo}$ exposed to NO fails to generate $S = {}^3/_2$ complexes in the presence or absence of benzoate (data not shown). The order of addition of benzoate and NO to $BZDO_{II}$ has no effect on the rhombicity or line width of complexes formed.

Because the amount of Fe(III) in the $BZDO_I$ approaches the $\alpha\beta$ subunit concentration, little or no $S = {}^3/_2$ signal was expected upon addition of NO to $BZDO_I$. Surprisingly, all of the mononuclear Fe(III) in $BZDO_I$ became reduced after exposure to NO to yield two sharp $S = {}^3/_2$ species identical to the NO complexes of $BZDO_{II}$ bound with benzoate (compare spectra a, e, and f in Figure 4). Such iron reduction has not been observed for other types of mononuclear iron-containing enzymes, and the mechanism is not yet understood. Quantification of all $S = {}^3/_2$ species yields 0.6 ± 0.1 spin/$\alpha\beta$, consistent with the total mononuclear iron content. Iron reduction upon NO addition is also observed for benzoate-free $BZDO_I$ samples prepared by buffer exchange. However, as shown in Figure 4g, only a single $S = {}^3/_2$ species with line width ~30 G and $E/D = 0.012$ similar to that of (benzoate free) $BZDO_{II}$−NO is generated. Addition of benzoate to the benzoate-free $BZDO_I$−NO sample generates the same spectrum as seen for the $BZDO_{II}$−NO−benzoate and $BZDO_I$−NO samples (not shown).

Multiple species are often observed in the nitrosyl complexes of mononuclear iron-containing proteins, which might reflect either lack of saturation of the active site with substrate, different types of metal sites, or different binding modes of the substrate in the active site. Figure 5A shows that the EPR signal of the $E/D = 0.012$ species disappears and that of the signal of the $E/D = 0.029$ species increases as benzoate is added to $BZDO_{rec}$. This conversion maximizes when the substrate and the occupied mononuclear Fe(II) sites are approximately equal in concentration, suggesting that benzoate binds tightly to the Fe(II)−NO complex. Since the two species remain in a 2:1 ratio at the end of the titration,

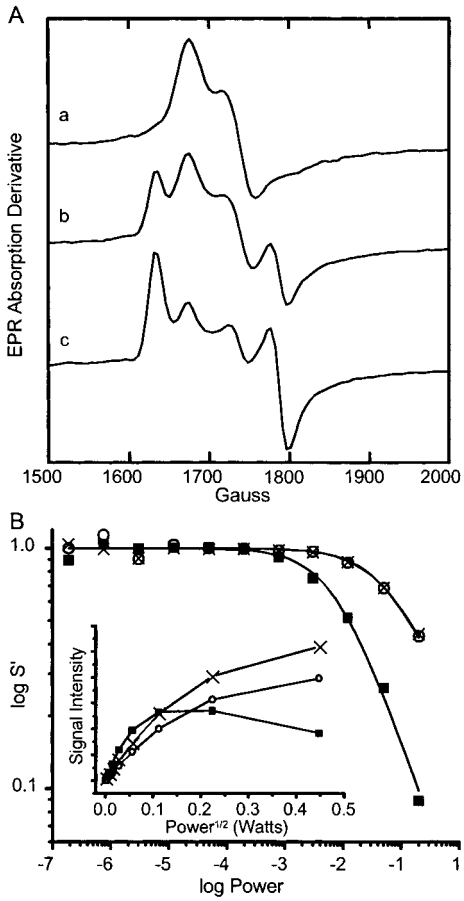

FIGURE 5: Characterization of the ternary BZDO−substrate−nitrosyl complex. (Panel A) Benzoate was added to $BZDO_{rec}$ (250 μM sites) followed by exposure to NO: (a) no benzoate; (b) 50 μM benzoate; (c) 250 μM benzoate. (Panel B) Saturation behavior of the signals shown in panel A plotted and analyzed as described in Materials and Methods. (■) $E/D = 0.012$ signal of substrate-free enzyme, (○) $E/D = 0.012$ signal of substrate-bound enzyme, and (×) $E/D = 0.029$ signal of the substrate-bound enzyme. Inset: Plot of the EPR signal intensity of the same species versus the square root of the microwave power. Instrument conditions: temperature, 4 K; modulation amplitude, 10 G; microwave frequency, 9.63 GHz.

either (i) only about two-thirds of the Fe(II)−NO binds benzoate to form the $E/D = 0.029$ complex or (ii) the mononuclear iron binds benzoate to form two electronically different ternary complexes in a 2:1 ratio, one of which has the same E/D as the substrate-free nitrosyl complex. These possibilities can be distinguished by measuring the microwave power saturation behavior of the spectra. Figure 5B shows a plot of the normalized signal intensity at 4 K versus microwave power (log scale) of the $E/D = 0.012$ species in the absence and presence of benzoate and the $E/D = 0.029$ species observed only in the presence of benzoate. Fits to the data using eq 1 gave $P_{1/2}$ values of 7 mW ($b = 1.4$) for the $E/D = 0.012$ species of $BZDO_{rec}$−NO and 45 mW ($b = 1$) for both the $E/D = 0.012$ and 0.029 species of substrate-bound $BZDO_{rec}$−NO. Figure 5B inset shows a plot of the signal intensity of these species versus the square root of the microwave power. From the shape of the curves at high powers, it is clear that the nitrosyl complexes of the enzyme and enzyme−substrate complex exhibit different relaxation mechanisms. When only the $E/D = 0.012$ species in the presence and absence of benzoate are compared, the satura-

[3] The complex signals near $g = 2$ in Figures 4d−g and 6e,f are assigned to dinitrosyl−iron complexes formed from the Rieske cluster interacting with NO. This assignment is supported by the observation that reactions of $BZDO_{apo}$ with NO generate identical EPR spectra (data not shown) and exposure of NO to other iron−sulfur-containing proteins yields these complexes (*28*, *29*).

Table 5: Single Turnover of *P. putida* mt-2 Benzoate 1,2-Dioxygenase[a]

		benzoate *cis*-diol yield			
reaction	electrons added[b]	nmol of product	product/ $\alpha\beta$	product/ mono Fe[c]	product/ mono Fe(III) generated[d]
$BZDO_{II}$ as isolated[e]	0	0.6	0.01	0.01	
+benzoate + O_2	0	0.8	0.02	0.03	
reduced $BZDO_{II}$					
+benzoate + O_2	1	23.7	0.47	0.59	1.04
+Fe(II)	1	27.7	0.55	0.55[f]	
+oxidized BZDR	1	29.2	0.58	0.73	
+reduced BZDR	4	61.0	1.22	1.53	
reduced BZDR					
+benzoate + O_2	3	0.0	0.0	0.0	

[a] Reactions were performed as described in Materials and Methods. Each reaction was performed three to six times using BZDO purified by method II [50 nmol of $BZDO_{II}$ ($\alpha\beta$), ~0.8 mononuclear Fe/$\alpha\beta$]. The standard error for each reaction was less than 8%. [b] For all $BZDO_{II}$ reactions, neither the electron associated with the mononuclear Fe(II) site nor the added Fe(II) is counted as an added electron. The number of electrons added is entirely based on full reduction of the theoretical number of reducible cofactors in the reaction ($BZDO_{II}$ = 1, BZDR = 3). [c] Normalized to the mononuclear Fe(II) originally present in the sample. [d] Normalized to the mononuclear Fe(III) generated during turnover by quantification of the majority EPR species with E/D = 0.115. [e] $BZDO_{II}$ as isolated indicates the enzyme after purification without addition of benzoate or O_2 prior to denaturation of the enzyme and product analysis. All other reactions were initiated with the addition of benzoate and O_2. [f] Because exogenous iron was added to the reaction, the mononuclear iron content used in this calculation was assumed to be 1.0.

tion data suggest that, despite identical rhombicities, the two species represent two different complexes. Thus, it appears that, with excess benzoate present, the E/D = 0.012 and 0.029 species represent two different substrate-bound complexes and that, in the presence of substrate, the system has an additional spin relaxation pathway.

Single Turnover Reaction. The single turnover results summarized in Table 5 show that BZDO is capable of catalyzing the oxygenase chemistry of the entire BZDOS. At the limit of experimental detection, $BZDO_{II}$ as isolated appears to have a small amount of product bound. This is not increased by further exposure of the enzyme to benzoate and oxygen despite the fact that the mononuclear iron is reduced and could potentially bind oxygen. Only when both the Rieske cluster and mononuclear iron are in the reduced states is $BZDO_{II}$ capable of catalyzing a single turnover of the reaction cycle. The product yield of different enzyme batches ranged from 25% to 47% per $\alpha\beta$ protomer and correlated reasonably well with the mononuclear Fe content of the particular preparation. Accordingly, Table 5 shows that increasing the occupancy of the mononuclear iron site by addition of Fe(II) to the reaction increases the product yield by 17%. When normalized to the mononuclear iron occupied $\alpha\beta$ protomer content, the yield is 55−60%. This yield is somewhat lower than we recently reported for the NDO class of Rieske dioxygenase (85−99%) (*7*). Using the spectroscopic approaches described below, it is possible to quantitate the amount of mononuclear iron actually oxidized during a single turnover. This value correlates with the yield of benzoate *cis*-diol (104% yield), clearly indicating that BZDO can catalyze the coupled reaction in high yield in the absence of BZDR.

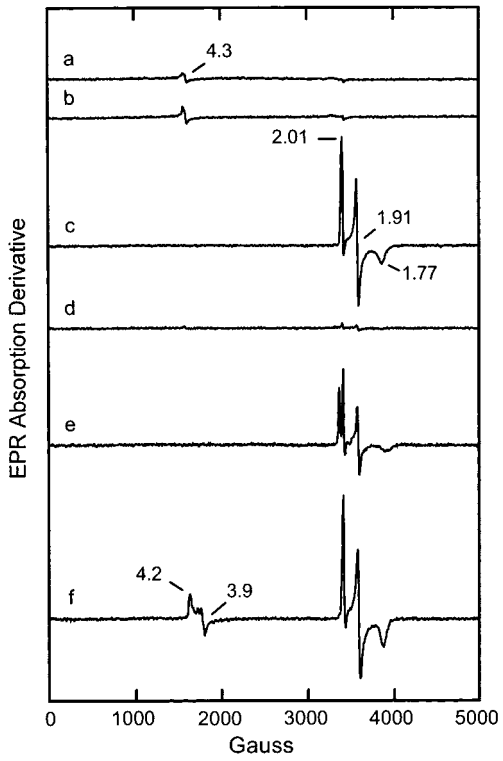

FIGURE 6: Regulation of the binding of O_2 and NO to BZDO. The EPR spectra of $BZDO_{II}$ (205 μM sites) in the presence of 10 mM benzoate before (a) and after (b) exposure to 2 atm of O_2 for 30 min at 23 °C. Also shown are spectra of reduced $BZDO_{II}$ before (c) and after (d) a 30 min reaction with O_2 at 23 °C in the absence of benzoate. Spectra e and f are of reduced $BZDO_{II}$ exposed to NO in the absence and presence of 10 mM benzoate, respectively. Instrument conditions: (a, b) microwave power, 100 μW; temperature, 2 K; modulation amplitude, 10 G; microwave frequency, 9.63 GHz; (c−f) temperature, 10 K.

Addition of 1 equiv of oxidized BZDR to the BZDO single turnover reaction increases the yield per $\alpha\beta$ about 20%, which may be related to the ability of BZDR to redistribute electrons between partially and fully populated active sites (see below). Addition of reduced BZDR to the single turnover reaction increases the yield of benzoate *cis*-diol above 100%, consistent with the additional electrons it can introduce into the reaction. Reduced BZDR alone is incapable of catalyzing benzoate hydroxylation.

Regulation of Oxygen Reactivity. Exposure of $BZDO_{II}$ with a reduced mononuclear iron and an oxidized Rieske cluster to O_2 in the presence of benzoate causes little oxidation of the mononuclear iron as shown in Figure 6a,b. After a 30 min incubation with O_2, none of the characteristic E/D = 0.076 EPR-detectable species of active site Fe(III) is apparent in the sample. A small increase in the E/D = 0.33 Fe(III) species occurs, but quantification of this signal shows that it accounts for less than 2% of the mononuclear iron. Thus, even when benzoate is bound, the ferrous ion of $BZDO_{II}$ does not readily react with O_2 to yield an EPR-active species. It is possible that oxygen might bind to form an Fe(III)−superoxo species or similar EPR-silent species. However, such a species would be readily apparent in the Mössbauer spectrum of the complex, but no species other than Fe(II) was detected.

Reduction of the Rieske cluster of $BZDO_{II}$ creates an enzyme form containing two electrons available for catalysis

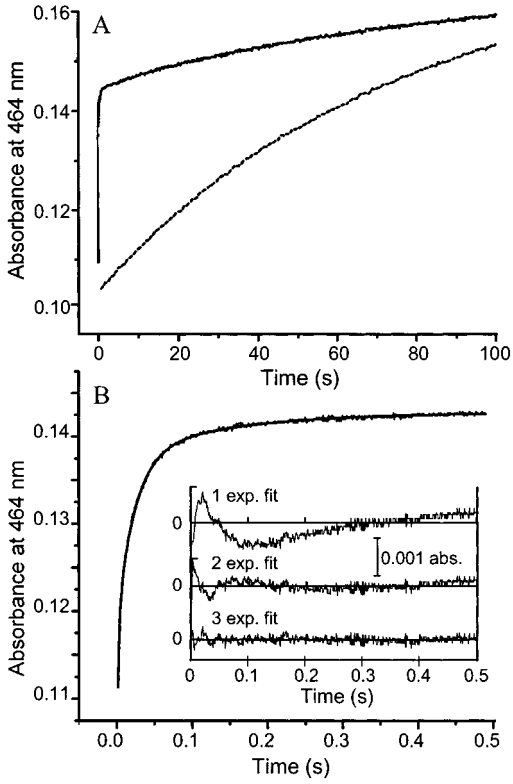

FIGURE 7: Single turnover of reduced BZDO monitored by stopped-flow optical spectroscopy. $BZDO_{II}$ (60 μM sites) was reduced stoichiometrically with dithionite and 100 μM methyl viologen and rapidly mixed (1:1) with oxygenated buffer (~1.8 mM O_2 at 4 °C) with or without substrate. The reactions were carried out at 4 °C in 50 mM MOPS buffer, pH 6.9, as described in Materials and Methods. Panel A: Kinetic time courses of the reaction monitored at 464 nm are shown for the reactions in the presence (solid line) and absence (dotted line) of 1 mM benzoate. Panel B: The first 500 ms of the reaction in the presence of benzoate and the residual errors from nonlinear regression fits using one, two, and three summed exponential time courses, respectively, showing that a three-exponential fit is required (see Table 6). The slow (fourth) exponential phase with a relaxation time 0.013 s^{-1} evident in the main figure at times beyond 1 s contributes very little to the time course in this time domain. The three-exponential fit is superimposed on the data as a solid line.

in each active site. However, spectra c and d of Figure 6 show that, after addition of O_2 to reduced, benzoate-free $BZDO_{II}$, no significant oxidation of the mononuclear iron occurs, and only slow oxidation of the Rieske cluster occurs. In contrast, rapid oxidation of both centers is observed when benzoate is added (see below).

A similar pattern of reactivity is observed using NO as an oxygen analogue. Figure 6e shows the EPR spectrum of benzoate-free BZDO after addition of NO to the enzyme containing reduced Rieske clusters. No EPR-active $S = {}^3/_2$ species is formed, indicating that NO has not formed a stable 1:1 complex with the ferrous ion.[3,4] In contrast, addition of benzoate to reduced BZDO in the presence of NO (Figure 6f) leads to the formation of the $S = {}^3/_2$ species, indicating that even when electrons are available, substrate must be bound before NO (and, by inference, O_2) can bind to the mononuclear iron. The $S = {}^3/_2$ species of the reduced ternary complex are similar to those of the ternary complex with an oxidized Rieske cluster (Figure 4e,f) except that the $E/D = 0.012$ species is nearly lost, and a second rhombic species is formed with E/D very close to 0.029. This suggests that small changes occur at the mononuclear site as the Rieske cluster is reduced, but two mononuclear iron−substrate complexes are still present.

[4] An alternative explanation in which two molecules of NO are bound to form an $S = 1$ or 3 species is unlikely because no signals from integer spin systems are observed near $g = 4$ or 12 in parallel mode EPR experiments.

Table 6: Reciprocal Relaxation Times for Single Turnover Reactions of *P. putida* mt-2 Benzoate 1,2-Dioxygenase

substrate	$1/\tau_1$ (amp)[a]	$1/\tau_2$ (amp)	$1/\tau_3$ (amp)	$1/\tau_4$ (amp)
none				0.013 (100)
benzoate	260 (36)	39 (28)	6.7 (7)	0.013 (29)
3-F-benzoate	47 (42)	8.9 (27)	0.51 (6)	0.013 (25)
3-Me-benzoate	23 (40)	4.9 (31)	0.38 (6)	0.013 (23)
3-Cl-benzoate	7.1 (28)	2.3 (31)	0.30 (9)	0.013 (32)

[a] Observed amplitude in percent of total change for the first four exponential phases of the reaction. When substrates are present, a fifth very slow, apparently nonexponential phase is also observed which accounts for about 20% of the total absorbance.

Kinetics of Oxygen Reactivity. The effect of benzoate on the rate of reaction of reduced BZDO with O_2 is shown more quantitatively using stopped-flow spectrophotometry. Figure 7 shows the increase in optical absorption upon oxidation of the Rieske cluster after stoichiometrically reduced $BZDO_{II}$ is rapidly mixed with O_2 in the presence or absence of benzoate at 4 °C. Since both benzoate and oxygen were supplied in sufficient excess to establish pseudo-first-order conditions and only one turnover could occur in the absence of excess reductant, the time course should be fit by a sum of one or more exponential phases. Accordingly, the time course of the absorbance change occurring for the slow reaction in the absence of benzoate is fit well by a single exponential with a reciprocal relaxation time of $1/\tau_1 = 0.013 \pm 0.001$ s^{-1}. This value is much smaller than the turnover number of the enzyme at 4 °C (4.5 s^{-1}) with all components saturated, and thus it is not relevant to the natural turnover cycle. Oxidation of reduced $BZDO_{II}$ in the presence of substrate occurs much more rapidly (see Figure 7). Over the first 100 s, the time course displays four-phase kinetics with the relaxation times and relative amplitudes listed in Table 6. The first three phases are kinetically competent and represent the same fraction of enzyme oxidized as product produced for a particular batch of BZDO. The slowest phase has the same reciprocal relaxation time as observed for the substrate-free reaction, and thus it may represent spontaneous oxidation of the Rieske cluster without product formation. An additional very slow oxidation of the Rieske cluster accounting for about 20% of the total absorbance change is also observed at longer times than shown in Figure 7. The origin of this phase is unknown, but it is observed only in the case when substrates are present. Although benzoate *cis*-diol is unstable in the acidic or basic solutions necessary for very rapid chemical quench procedures for this enzyme, slower heat denaturation quenching shows that all product is formed in the first 10 s of the reaction. Thus, the rapid phases of the oxidation reaction of the Rieske cluster are likely to be correlated with product formation.

Rapid scan optical spectra of the reaction shown in Figure 8 do not reveal an intermediate with a unique optical

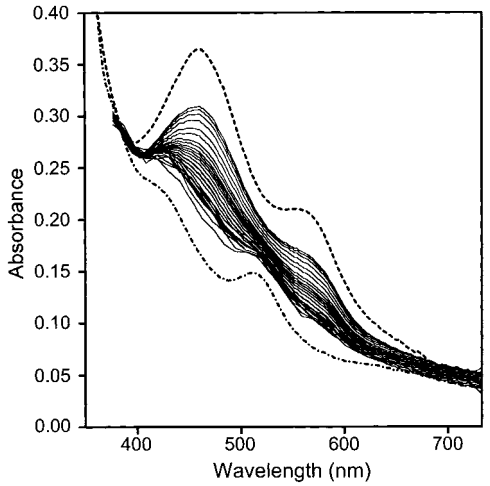

FIGURE 8: Rapid scan stopped-flow spectra of the BZDO single turnover reaction with benzoate and O_2. The reaction was initiated as described in Figure 7, except that 100 μM $BZDO_{II}$ (sites, before mixing) was used. The first (lowest) trace was recorded at 1.28 ms after mixing. Selected traces to a maximum (highest trace) of 600 s are shown. Superimposed on the figure are the optical spectra of 50 μM BZDO with the Rieske cluster in the fully reduced (-·-) and oxidized (- - -) states. For these spectra, the mononuclear iron is in the ferrous state. It becomes oxidized during the time course of a single turnover.

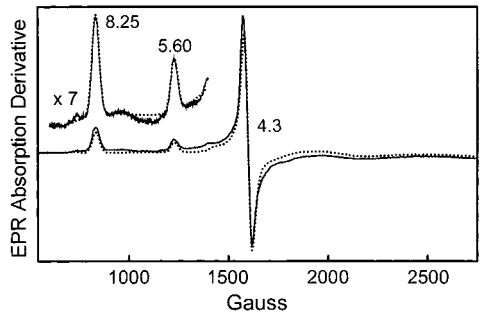

FIGURE 9: EPR spectrum of the BZDO single turnover reaction with benzoate and O_2. ^{57}Fe-enriched $BZDO_{II}$ (≈1 mM mononuclear iron sites) was reduced stoichiometrically with dithionite and 20 μM methyl viologen and mixed with an equal volume of oxygenated buffer containing 10 mM benzoate. The reaction was carried out in 100 mM MOPS buffer, pH 6.9, at 23 °C as described in Materials and Methods. After 60 s incubation the sample was frozen in liquid N_2. The spectrum shown was recorded at 20 K. The dotted line is a theoretical curve obtained by adding the simulations of the species with $E/D = 0.115$ (75%), $E/D = 0.33$ (20%), and $E/D = 0.235$ (5%). For the zero-field splitting parameters (D in cm^{-1}, E/D) we used (3.0, 0.115), (1.5, 0.33), and (1.5, 0.235). Conditions: microwave power, 200 μW; modulation amplitude, 9.8 G; microwave frequency, 9.63 GHz.

spectrum despite the observation of multiphase kinetics. The first spectrum recorded at 1.28 ms after mixing shows that a mixture of oxidized and reduced Rieske cluster is already present, consistent with the high rate constant for the first phase.

EPR and Mössbauer Analysis of BZDO Single Turnover. Reaction of reduced $BZDO_{II}$ with O_2 in the presence of benzoate results in a rapid decrease in the EPR signal of the reduced Rieske center near $g = 2$ and the appearance of new signals in the low-field region of the spectrum as shown in Figure 9. These spectral changes are complete within 10 s, in accord with the optical time course shown in Figures 7 and 8. Samples made after longer reaction times show a slow decrease in the intensity of the signal of the reduced Rieske cluster (requiring >30 min for full oxidation), indicating that Rieske oxidation occurs in both fast and very slow phases. The new signals in the low-field region derive from three distinct high-spin, mononuclear Fe(III) species, as shown in Figure 9. The spectra were obtained for a sample studied with Mössbauer spectroscopy, which showed that ca. 70% of the ^{57}Fe of the mononuclear site was in the ferric state. The majority species (75 ± 5% of Fe^{3+}) has $E/D = 0.115$ and contributes signals at $g_y = 8.25$ and $g_x = 3.35$ from the ground doublet and $g_z = 5.6$ from the middle doublet. A second species (ca. 20% of Fe^{3+}) has $E/D = 0.33$, yielding a resonance at $g = 4.3$ and a weak broader feature at $g = 9.7$. The third species (5% of Fe^{3+}) has $E/D = 0.235$ and yields signals at $g_z = 4.8$ and $g_x = 4.0$ from the middle doublet and a peak at $g_y = 9.3$ from the ground doublet. To determine the D-value of the $E/D = 0.115$ species, we have recorded spectra at 10 temperatures between 2.2 and 30 K. As the $g_y = 8.25$ and the $g_z = 5.6$ resonances belong to the ground and middle doublets, respectively, their intensity ratios change with temperature in a way determined by the value of D. Using spectral simulations that match the line shapes of the resonances at $g = 8.25$ and 5.6, we have varied D to obtain an optimal match over the whole temperature range, obtaining $D = +3.0 \pm 0.5$ cm^{-1}. (The background under these resonances was estimated by spectral simulations and by polynomial fitting.)

We have also recorded Mössbauer spectra of a sample of reduced BZDO (plus benzoate) enriched with ^{57}Fe in the mononuclear iron site after exposure to O_2 to induce a single turnover. A 4.2 K spectrum is shown in Figure 2b. About 30−40% of the original Fe(II) remained unreacted in this sample. The remainder of the iron has been oxidized to Fe(III) states. Further exposure to O_2 had no effect on the percent of Fe oxidized to the Fe(III) state. The major Fe(III) component is the species with $E/D = 0.115$. For $D = 3$ cm^{-1} about 85% of the molecules with $E/D = 0.115$ are in the $M_s = \pm^1/_2$ ground state. Its Mössbauer spectrum is readily simulated with the knowledge of D and E/D and taking into account that the magnetic hyperfine interactions of high-spin ferric complexes are generally isotropic, with A (in $AS{\cdot}I$ for $S = {}^5/_2$) approximately −27 to −29 MHz. The solid line drawn through the data of Figure 2b is a spectral simulation using the parameters from the last row of Table 4. Despite a considerable accumulation of data (1.2×10^7 counts/channel), the spectra are rather noisy, and therefore the precision of the analysis is rather limited. However, we obtained $A = -26.7 \pm 0.5$ MHz. (The spectrum of the ground Kramers doublet is quite insensitive to the z-components of the A-tensor and the quadrupole tensor. Thus, we obtained $A_x \approx A_y = -26.7$ MHz, with A_z undetermined.) We also have examined the EPR spectrum of this sample at 2 K. The ratio of the $E/D = 0.115$ and $E/D = 0.33$ species was the same as for the sample of Figure 9; however, the $E/D = 0.33$ species amounted to about 10% of the Fe(III) in the sample. Given the low concentration of the $E/D = 0.33$ and 0.235 species in the sample, their Mössbauer spectra are expected to be hidden in the noise. It is interesting to note that the spectra in Figure 2 seem to indicate that it is primarily the iron of the doublet with $\Delta E_Q = 3.1$ mm/s that has oxidized to the ferric form(s).

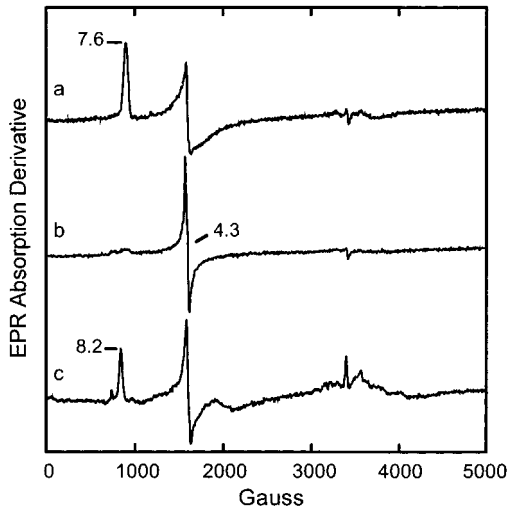

FIGURE 10: EPR spectra are of partially oxidized $BZDO_{II}$ (0.6 mM sites) (a) with no added ligands, (b) after the addition of 10 mM benzoate, or (c) after the addition of 5 mM benzoate *cis*-diol. After addition of the substrate or product, each sample was exposed to 2 atm of O_2 for 3 h, resulting in partial oxidation of the mononuclear iron. Instrument conditions: microwave power, 200 μW; temperature, 2 K; modulation amplitude, 10 G; microwave frequency, 9.63 GHz.

Ligand Exchange. The observation that the EPR spectrum of the mononuclear Fe(III) of $BZDO_{II}$ after a single turnover differs from that of $BZDO_I$ or $BZDO_I$ plus benzoate may indicate that product is bound in the active site of the former. Efforts to add the product to $BZDO_I$ failed to change the EPR spectrum even if the benzoate in this sample was first removed. One possibility is that the mononuclear iron must be in the ferrous state to allow efficient substrate or product binding from solution or their dissociation from the active site. This was examined by adding substrate or product to $BZDO_{II}$ and then oxidizing 10−20% of the mononuclear iron by prolonged exposure to 2 atm of O_2. The enzyme resists oxidation by this approach (see above), so this was the maximum amount of Fe(III) that could be obtained. Following this treatment, the enzyme in the absence of substrate or product (Figure 10a) exhibited an $E/D = 0.076$ species identical to that observed for $BZDO_I$. This supports the notion introduced above that this species derives from mononuclear Fe(III) in the substrate-free active site. Accordingly, when benzoate was present (Figure 10b), only the $E/D = 0.33$ species was observed, and the presence of product (Figure 10c) elicited the $E/D = 0.115$ species. These results indicate that, at the conclusion of a single turnover, BZDO appears to contain the oxidized Rieske cluster and mononuclear Fe(III) with benzoate *cis*-diol bound in the active site. Table 3 summarizes the EPR parameters of the mononuclear Fe(III) of BZDO in the different complexes.

Single Turnover of Alternate Substrates. Several different substituents in different positions can be added to the benzoate nucleus to form alternative substrates for BZDOS. The single turnover time courses for these substrates are significantly slower than for benzoate but still consist of multiple phases. The time courses for alternate substrates with F, Cl, and CH_3 substituents in the 3-position are shown in Figure 11A. These alternative substrates give relatively high turnover numbers (71%, 64%, and 47% of the wild-type turnover number for the 3-F-, 3-CH_3-, and 3-Cl-benzoates, respectively) and highly coupled reactions (each ≥88% coupled). At 4 °C, the reaction for each substrate over the first 100 s exhibits the very slow phase with a $1/\tau = 0.013$, like that observed in the time courses for the reactions of substrate-free and benzoate-bound reduced BZDO. Thus, this probably also represents spontaneous oxidation of the Rieske centers which cannot participate in a productive reaction. After subtraction of the small contribution of this phase to the first few seconds of the reaction, each of the time courses is fit well by three exponential phases (Figure 11B) with the rate constants shown in Table 6. At least two phases in each case are kinetically competent, and each phase is significantly slower than the corresponding phase in the benzoate oxidation time course.

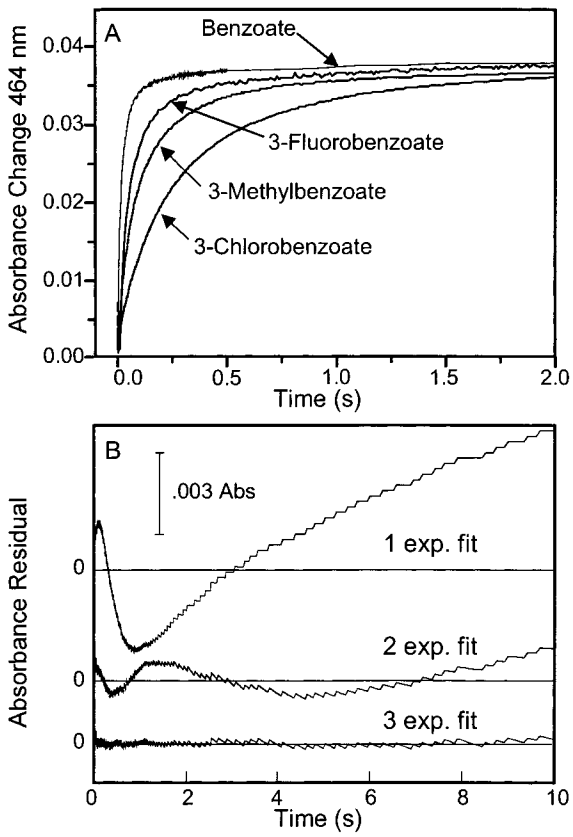

FIGURE 11: Single turnover reaction of reduced BZDO with alternative substrates monitored by stopped-flow optical spectroscopy. (A) $BZDO_{II}$ (60 μM sites) was reduced stoichiometrically with dithionite and 100 μM methyl viologen and rapidly mixed (1:1) with oxygenated buffer (~1.8 mM O_2 at 4 °C) containing the substrate indicated on the figure at 2 mM concentration (before mixing). The reactions were carried out at 4 °C in 50 mM MOPS buffer, pH 6.9, as described in Materials and Methods. Each reaction time course exhibited a very slow phase with a reciprocal relaxation time of 0.013 s^{-1}, attributed to autoxidation of the Rieske cluster without product formation. For clarity, the minor contribution from this phase has been subtracted from the time courses shown. (B) Residuals from fitting the time course of the reaction using 3-Cl benzoate as the substrate with one, two, and three exponential phases, respectively. Analysis of the other time courses shown in (A) also required three exponentials for a satisfactory fit.

DISCUSSION

It has been shown here that the reduced BZDO component isolated from *P. putida* mt-2, in the absence of its reductase component, is capable of a single turnover to produce a high yield of the *cis*-dihydroxylated product. This shows that the

chemical reactions occur on the BZDO component and must, therefore, involve the mononuclear iron and/or Rieske iron sulfur centers of that component. The current studies show that the rate of the product-forming reaction exceeds the enzyme turnover number, demonstrating that BZDO catalyzes the oxidation reaction at least as fast as the complete BZDOS. Thus, in accord with our previous studies of the NDOS subclass of Rieske dioxygenase (*7*), the benzoate subclass also does not require component interactions or electron transfer from external sources during the catalytic cycle to catalyze oxygenase chemistry. Given the similarities in spectroscopic properties and chemical reactions of the Rieske dioxygenase subclasses, it seems likely that this will be generally true for the entire family, despite the structural differences that have been noted.

The BZDOS offers significant new insight into catalysis by Rieske dioxygenases because it can be stablized with the mononuclear iron in either the oxidized or reduced form so that substrate interactions can be evaluated in each state. This is facilitated by the fact that the mononuclear iron is in an asymmetric electronic environment, which gives the resulting EPR spectrum much greater sensitivity to structural changes than observed for other Rieske dioxygenases. Also, the comparatively high substrate solubility and the ability to utilize alternative substrates have allowed the kinetics of the single turnover reaction to be examined over the entire kinetic time course for the first time. An unexpected complexity is revealed by this analysis that is discussed in the following sections.

Comparison with NDO Single Turnover. Despite the fact that NDOS requires an additional ferredoxin component, both the minimum requirements for turnover and the regulation of catalysis appear to be very similar to those reported here for BZDOS. For each enzyme, single turnover occurs only when both the Rieske and mononuclear iron sites are reduced, substrate is bound, and the oxygenase is exposed to oxygen. For each system, when the Rieske cluster is reduced, the binding of NO (as an O_2 mimic) to the mononuclear iron apparently does not occur before substrate binds. This is remarkable in that NO can bind to the mononuclear iron in both enzymes in the absence of substrate when the Rieske cluster is oxidized, showing that the site is accessible. Moreover, the crystal structure of NDO with the Rieske cluster reduced suggests that the mononuclear iron is 5-coordinate and includes a solvent molecule (*23*, *30*). Thus, it could accommodate an NO ligand by either solvent displacement or a small shift in coordination geometry. While it is advantageous for the enzyme not to activate molecular oxygen in the absence of a substrate, the mechanism by which the NO (or O_2) is excluded from the iron remains unclear. The fact that it occurs in both enzyme systems, however, suggests that it is fundamental to the regulatory scheme of this enzyme family. It is possible that substrate creates a binding site near the iron for small molecules or that it in some way lowers the redox potential of the mononuclear iron site to facilitate oxygen and NO binding as we have described for other classes of dioxygenases (*31*, *32*). However, the crystal structure of NDO strongly suggests that this is not accomplished by direct coordination of the substrate to the iron (*3*).

The overall yield of product from a single turnover is somewhat lower in the case of BZDO than we have reported for NDO (*7*). The yield per occupied mononuclear site of NDO approaches 100% while in no case have we observed greater than 75% yield for BZDO even when the mononuclear site is reconstituted with added Fe(II). Nevertheless, the yield is sufficient in both cases to state with confidence that the oxygenase component is solely responsible for substrate oxygenation. For both NDO and BZDO, we have shown that one-electron oxidation of a Rieske cluster and a mononuclear iron is required for product formation, thus establishing that a Rieske−mononuclear iron pair represent the catalytic unit. Integration of the EPR spectra for the reduced oxygenase components shows that the Rieske center occupancy is usually close to 100% in the case of NDO, but it is more variable in the case of BZDO. Consequently, at least part of the lower yield of the latter system may derive from inactivity of sites without Rieske clusters. In the case of NDO, the yield could be brought to 100% on the basis of the electrons present in the system by adding the oxidized NDF ferredoxin component, presumably because this component can redistribute electrons from Rieske clusters that do not have a mononuclear iron partner to fully functional active sites (*7*). While a higher yield was also observed when the oxidized BZDR reductase component was added in the BZDO single turnover, the yield remained lower than 100%. If, as appears to be the case, BZDR combines the roles of the NDR and NDF components, then it may be able to similarly redistribute electrons and increase the single turnover yield from sites that are missing a mononuclear iron. However, if a Rieske cluster is missing from an active site, an electron in the mononuclear iron center may not be accessible to BZDR and therefore may not contribute to the single turnover yield. Indeed, following a single turnover, Mössbauer spectroscopy indicates that about 30% of the mononuclear iron remains in the reduced state for the samples investigated and the amount of oxidized mononuclear iron correlates with the product yield.

Importance of Redox State in Substrate and Product Interaction with the Mononuclear Iron of BZDO. The results reported here support the hypothesis that the mononuclear iron must be in the reduced state for product to rapidly dissociate or substrate to bind. $BZDO_I$ in the presence or absence of benzoate exhibits an EPR spectrum dominated by an $E/D = 0.076$ Fe(III) species. While it is possible that substrate causes no spectroscopic change when it binds in the active site, this seems unlikely. Indeed, we show here (Figure 10) that three quite different EPR spectra result from oxidizing the $BZDO_{II}$ Fe(II) site in the presence of benzoate, *cis*-diol benzoate, or when no substrate or product is present, suggesting that the iron environment is very sensitive to small molecule binding. In this experiment, the $E/D = 0.076$ species is specifically observed when no substrate or product is present. Consequently, the $E/D = 0.076$ species of $BZDO_I$ is proposed to derive from the substrate-free Fe(III) mononuclear site, and we hypothesize that $BZDO_I$ has little benzoate in the active site despite its presence in solution. In contrast, addition of benzoate to the Fe(II)-containing $BZDO_{II}$ causes significant changes in both the electronic environment and relaxation behavior of the mononuclear metal center as detected by EPR spectroscopy of the nitrosyl complex. Thus, we conclude that benzoate has ready access to the active site when the mononuclear iron is reduced. The same conclusion can be reached by considering that the novel

$E/D = 0.115$ Fe(III) species is only observed when the mononuclear Fe(II) centers are oxidized in the presence of product or after a single turnover when product is formed in the active site. It is specifically not observed when product is added to the Fe(III)-containing $BZDO_I$, suggesting again that reduction of the mononuclear iron center is necessary for small molecule exchange. Accordingly, product is not recovered in high yield after a single turnover until the enzyme is denatured. These observations suggest that reduction of the Fe(III) center at the end of the turnover cycle is important for product release. In effect, electron transfer from external components completes the catalytic cycle rather than initiating it as commonly thought. If this sequence is correct, then it implies an important catalytic role for BZDR, beyond simple electron transfer; namely, BZDR must bind and rereduce the BZDO component before product release and the beginning of a new cycle. A role for conformational change linked to the oxidation state of the mononuclear iron in the regulation of catalysis is also implied by this observation. This may have a bearing on the observed reaction kinetics as discussed below.

Kinetics of Single Turnover. The time course of the single turnover reaction is followed in the studies described here primarily as a change in the absorbance of the Rieske cluster upon its oxidation. The results clearly show that the highest rate constant for this part of the reaction exceeds the overall turnover number (4.5 s^{-1}) by 50-fold. Indeed, the reciprocal relaxation times of each of the phases that cannot be attributed to simple autoxidation of the Rieske cluster exceed the turnover number. This suggests that a later reaction, perhaps attack of activated oxygen on the substrate or product release in association with the transfer of electrons from BZDR, is rate limiting. Unfortunately, most of these reactions are likely to give relatively weak chromophoric changes, and thus far, no evidence for species beyond the oxidized and reduced Rieske cluster has been detected in the rapid scan optical spectra of the single turnover reaction. The transient kinetic studies indicate that, in the absence of substrate, both the Rieske and mononuclear iron sites are essentially unreactive with O_2 on the time scale of turnover. These observations demonstrate that the rapid transfer of an electron from the Rieske center is intimately tied to the reaction of the enzyme with substrate and oxygen.

Single Turnover of Alternative Substrates. The use of alternative substrates significantly decreases the rates of both single and multiple turnover reactions, but the effect on the single turnover reaction kinetics is greater. From the limited set of alternative substrates investigated with transient enzyme kinetic techniques thus far, no clear trend emerges to allow the correlation of rate with electrophilicity or bulk of the new substituents. These studies are complicated by the tendency of the alternative substrates to uncouple the reaction, leading to reduction of O_2 without substrate oxidation. The alternative substrates with new substituents in the 3-position were selected for the initial study reported here because they cause the least uncoupling.

The use of alternative substrates shows that the observed reciprocal relaxation times for all fast phases in the single turnover time course are dependent on the specific substrate present. This suggests that the substrate plays a direct role in the reaction in which the Rieske cluster is oxidized. This might involve structural alterations in the electron transfer pathway between the metal centers, or it may mean that attack on substrate occurs simultaneously with the transfer of an electron from the Rieske cluster. Although the latter proposal is attractive, the lack of a correlation between the reaction rate and bulk or electronic property of the substituent does not support it. Another possibility is that the substrate itself forms part of the electron transfer pathway, thereby accounting for the observation that it must be present before oxygen activation occurs. However, a reasonable electron transfer pathway between the Rieske cluster and the mononuclear iron site involving Asp205 in the case of NDO has been recognized and tested convincingly via site-directed mutagenesis (*23*, *33*).

A second potentially significant observation from the single turnover reactions of both benzoate and the alternative substrates is that three relatively fast exponential phases are required to fit the time course in addition to the very slow phase correlated with autoxidation. One interpretation of this observation is that three sequential steps occur in the product-forming reaction. However, no intermediates with distinguishable spectra were observed, and it is difficult to conceive of a mechanism in which a single electron is transferred in three sequential, substrate-dependent reactions from a single iron−sulfur cluster with indistinguishable spectral changes. One alternative is that the enzyme preparation has three different subpopulations due to partial inactivation or related phenomena. While this cannot be ruled out, the fact that many batches of enzyme exhibit similar kinetics argues against it. Another possibility is that the reaction occurs at different rates for each of the three active sites in a given enzyme molecule. This might be a result of a static structure of the enzyme that makes the three sites inequivalent in some way. Alternatively, a dynamic structural change may occur during each cycle, allowing each active site to react in turn. The inequivalence of the sites is supported by the observation of two different species in both the Mössbauer spectra of $BZDO_{rec}$ and the EPR spectra of the enzyme−substrate−NO complex. These alternatives can be probed by more extensive kinetic studies, which are in progress.

Relevance to Mechanism. On the basis of the results reported here and those of our previous study of NDOS, a consensus mechanism emerges that invokes the utilization of the two reducing equivalents held in the two metal sites of the fully reduced Rieske dioxygenase active site to activate molecular oxygen and catalyze substrate dihydroxylation (Scheme 2). Participation of the other component(s) is important only after the chemistry is complete in order to allow the product to be released and the enzyme to be primed for another cycle. The studies reported here show directly that the Fe(III) product species predominates at the end of a single turnover cycle because no reduced reductase component is present to initiate product release.

If only two electrons are involved in the oxygen activation process, then it is possible that either an Fe(III)−peroxo or an Fe(V)−oxo species provides the reactive form of oxygen required for the reaction (*7*). Both of these forms have also been implicated from recent work using model inorganic chelate systems (*34*), and the involvement of an Fe(III)−peroxo intermediate has also been invoked from kinetic isotope effect studies of the Rieske monooxygenase enzyme PMO (*35*). While the primary reactions of PMO and BZDO

Scheme 2: Proposed Catalytic Cycle for Benzoate 1,2-Dioxygenase Emphasizing the Role of BZDR To Reduce the Enzyme at the Completion of the Chemical Transformation To Allow Product Release

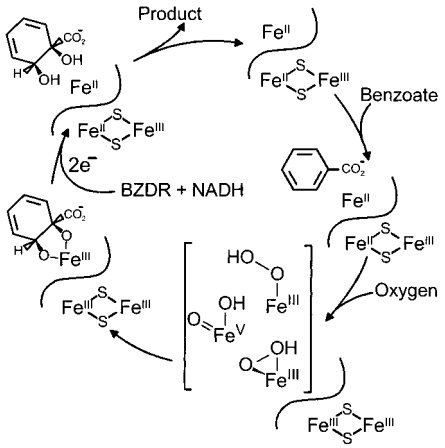

differ, both the Mössbauer and EPR characteristics of the enzymes are very similar in all of the oxidation states of the mononuclear iron and Rieske cluster studied thus far (*36*−*39*). Indeed, BZDO is spectroscopically more similar to PMO than to any of the Rieske dioxygenases. Thus, it is possible that the oxygen activation phases of these enzymes proceed along a similar track and diverge only at the stage of the actual oxygen insertion reaction itself.

A new aspect of the mechanism of Rieske dioxygenases that has emerged from this study is that the rate of the electron transfer reaction between the metal centers depends on the presence of the organic substrate and its nature. This may mean that the view expressed above, conceiving of the reactive species as involving only iron and some form of activated oxygen, may be too simplistic. Future studies are necessary using the broad range of substrates accommodated by this enzyme class, as well as the diversity of types of oxygenase and oxidase reactions they catalyze, to probe this intriguing possibility. Finally, the preliminary evidence presented here showing that there are three distinct reactions during a single turnover suggests that the trimeric structure of the enzyme may play an unexpected role in the catalytic cycle. This role can be explored using analogues of the numerous site-directed mutations near the subunit boundaries that have been recently reported for the mechanistically similar enzyme NDO (*33*, *40*).

REFERENCES

1. Gibson, D. T., and Parales, R. E. (2000) *Curr. Opin. Biotechnol. 11*, 236−243.
2. Resnick, S. M., Lee, K., and Gibson, D. T. (1996) *J. Ind. Microbiol. Biotechnol. 17*, 438−457.
3. Carredano, E., Karlsson, A., Kauppi, B., Choudhury, D., Parales, R. E., Parales, J. V., Lee, K., Gibson, D. T., Eklund, H., and Ramaswamy, S. (2000) *J. Mol. Biol. 296*, 701−712.
4. Tierney, D. L., Gassner, G. T., Luchinat, C., Bertini, I., Ballou, D. P., and Penner-Hahn, J. E. (1999) *Biochemistry 38*, 11051−11061.
5. Gassner, G. T., Ballou, D. P., Landrum, G. A., and Whittaker, J. W. (1993) *Biochemistry 32*, 4820−4825.
6. Pavel, E. G., Martins, L. J., Ellis, W. R., Jr., and Solomon, E. I. (1994) *Chem. Biol. 1*, 173−183.
7. Wolfe, M. D., Parales, J. V., Gibson, D. T., and Lipscomb, J. D. (2001) *J. Biol. Chem. 276*, 1945−1953.
8. Batie, C. J., LaHaie, E., and Ballou, D. P. (1987) *J. Biol. Chem. 262*, 1510−1518.
9. Ballou, D. P., and Batie, C. (1988) in *Oxidases and Related Redox Systems* (King, T. E., Mason, H. S., and Morrison, M., Eds.) pp 211−226, Alan R. Liss, New York.
10. Batie, C. J., and Ballou, D. P. (1990) *Methods Enzymol. 188*, 61−70.
11. Yamaguchi, M., and Fujisawa, H. (1978) *J. Biol. Chem. 253*, 8848−8853.
12. Yamaguchi, M., and Fujisawa, H. (1980) *J. Biol. Chem. 255*, 5058−5063.
13. Yamaguchi, M., and Fujisawa, H. (1982) *J. Biol. Chem. 257*, 12497−12502.
14. Reiner, A. M., and Hegeman, G. D. (1971) *Biochemistry 10*, 2530−2536.
15. Cohen-Bazire, G., Sistrom, W. R., and Stanier, R. Y. (1957) *J. Cell. Comput. Physiol. 49*, 25−68.
16. Whittaker, J. W., Orville, A. M., and Lipscomb, J. D. (1990) *Methods Enzymol. 188*, 82−88.
17. Reiner, A. M. (1972) *J. Biol. Chem. 247*, 4960−4965.
18. Jeffrey, W. H., Cuskey, S. M., Chapman, P. J., Resnick, S., and Olsen, R. H. (1992) *J. Bacteriol. 174*, 4986−4996.
19. Fox, B. G., Froland, W. A., Dege, J. E., and Lipscomb, J. D. (1989) *J. Biol. Chem. 264*, 10023−10033.
20. Fish, W. W. (1988) *Methods Enzymol. 54*, 357−364.
21. Haigler, B. E., and Gibson, D. T. (1990) *J. Bacteriol. 172*, 457−464.
22. Haigler, B. E., and Gibson, D. T. (1990) *J. Bacteriol. 172*, 465−468.
23. Kauppi, B., Lee, K., Carredano, E., Parales, R. E., Gibson, D. T., Eklund, H., and Ramaswamy, S. (1998) *Structure 6*, 571−586.
24. Pikus, J. D., Studts, J. M., Achim, C., Kauffmann, K. E., Münck, E., Steffan, R. J., McClay, K., and Fox, B. G. (1996) *Biochemistry 35*, 9106−9119.
25. Fee, J. A., Findling, K. L., Yoshida, T., Hille, R., Tarr, G. E., Hearshen, D. O., Dunham, W. R., Day, E. P., Kent, T. A., and Münck, E. (1984) *J. Biol. Chem. 259*, 124−133.
26. Arciero, D. M., Lipscomb, J. D., Huynh, B. H., Kent, T. A., and Münck, E. (1983) *J. Biol. Chem. 258*, 14981−14991.
27. Chen, V. J., Orville, A. M., Harpel, M. R., Frolik, C. A., Surerus, K. K., Münck, E., and Lipscomb, J. D. (1989) *J. Biol. Chem. 264*, 21677−21681.
28. Woolum, J. C., Tiezzi, E., and Commoner, B. (1968) *Biochim. Biophys. Acta 160*, 311−320.
29. Radi, R. (1996) *Chem. Res. Toxicol. 9*, 828−835.
30. Karlsson, A., Parales, J. V., Parales, R. E., Gibson, D. T., Eklund, H., and Ramaswamy, S. (2000) *J. Inorg. Biochem. 78*, 83−87.
31. Lipscomb, J. D., and Orville, A. M. (1992) in *Metal Ions in Biological Systems* (Sigel, H., and Sigel, A., Eds.) Vol. 28, pp 243−298, Marcel Dekker, New York.
32. Orville, A. M., Lipscomb, J. D., and Ohlendorf, D. H. (1997) *Biochemistry 36*, 10052−10066.
33. Parales, R. E., Parales, J. V., and Gibson, D. T. (1999) *J. Bacteriol. 181*, 1831−1837.
34. Chen, K., and Que, L. (1999) *Angew. Chem., Int. Ed. Engl. 38*, 2227−2229.
35. Twilfer, H., Sandfort, G., and Bernhardt, F.-H. (2000) *Eur. J. Biochem. 267*, 5926−5934.
36. Bill, E., Bernhardt, F. H., and Trautwein, A. X. (1981) *Eur. J. Biochem. 121*, 39−46.
37. Bill, E., Bernhardt, F. H., Trautwein, A. X., and Winkler, H. (1985) *Eur. J. Biochem. 147*, 177−182.
38. Twilfer, H., Bernhardt, F. H., and Gersonde, K. (1981) *Eur. J. Biochem. 119*, 595−602.
39. Twilfer, H., Bernhardt, F. H., and Gersonde, K. (1985) *Eur. J. Biochem. 147*, 171−176.
40. Parales, R. E., Lee, K., Resnick, S. M., Jiang, H., Lessner, D. J., and Gibson, D. T. (2000) *J. Bacteriol. 182*, 1641−1649.

BI025912N